

Reconnaissance geochemical mapping of eastern South Greenland (60°30' to 62°30'N)

Agnete Steenfelt, Else Dam
and Peter Erfurt

Open File Series 92/10



December 1992

GRØNLANDS GEOLOGISKE UNDERSØGELSE
Ujarassiorput Kalaallit Nunaanni Misissuisoqarfiat
GEOLOGICAL SURVEY OF GREENLAND

GRØNLANDS GEOLOGISKE UNDERSØGELSE
Ujarassiorput Kalaallit Nunaanni Misissuisoqarfiat
GEOLOGICAL SURVEY OF GREENLAND
Øster Voldgade 10, DK-1350 Copenhagen K, Denmark

The Geological Survey of Greenland (GGU) is a research institute affiliated to the Mineral Resources Administration for Greenland (MRA) within the Danish Ministry of Energy. As with all other activities involving the non-living resources in Greenland, GGU's investigations are carried out within the framework of the policies decided jointly by the Greenland Home Rule Authority and the Danish State.

Open File Series

The Open File Series consists of unedited reports and maps that are made available quickly in limited numbers to the public. They are a non-permanent form of publication that may be cited as sources of information. Certain reports may be replaced later by edited versions.

Citation form

Open File Series Grønlands Geologiske Undersøgelse

conveniently abbreviated to:

Open File Ser. Grønlands geol. Unders.

GGU's Open File Series består af uredigerede rapporter og kort, som publiceres hurtigt og i et begrænset antal. Disse publikationer er midlertidige og kan anvendes som kildemateriale. Visse af rapporterne vil evt. senere blive erstattet af redigerede udgaver.

ISSN 0903-7322

GRØNLANDS GEOLOGISKE UNDERSØGELSE
Open File Series 92/10

Reconnaissance geochemical mapping of eastern South Greenland
($60^{\circ}30'$ to $62^{\circ}30'$ N)

Agnete Steenfelt, Else Dam and Peter Erfurt

December 1992

Abstract

Geochemical mapping based on fine fraction of stream sediments and stream waters has been carried out along the east coast of South Greenland. 145 samples were collected in the ice free strips of land in the fjord section between $60^{\circ}30'$ to $62^{\circ}30'N$, corresponding to an average sampling density of 1 sample per 70 km^2 (including ice covered areas between the fjords). The spatial element distributions outline lithogeochemical and metallogenic provinces correlatable with provinces recognised in an earlier geochemical survey of western South Greenland. Stream sediment anomalies for Au, Cu, Zn, U and W cluster around Danell and Lindenow Fjords, and detailed exploration is recommended in this region.

Introduction

The geochemical survey carried out in eastern South Greenland is part of the Geological Survey of Greenland's geochemical mapping programme based on drainage samples. The purpose of this programme is to provide reconnaissance geochemical data which may be used together with geophysical and geological information to outline provinces or zones with potential for mineral resources.

Samples were collected in the period of 6th to 18th July 1992 by P. Erfurt and E. Hansen who took part in GGU's 'Suprasyd' programme (Nielsen et al., in review). An AS 350 (Ecureuil) helicopter temporarily based at Prins Christian Sund Telestation was used for transportation.

The geochemical survey was financed by the Mineral Resource Administration for Greenland (MRA) under the Danish Ministry of Energy. Administratively, the surveyed area belongs to the municipality of Tasiilaq except for the south coast of Lindenow Fjord which belongs to Nanortalik.

Geological setting

The sampled area lies within the Proterozoic Ketilidian mobile belt of the Laurentian shield and includes a small part of the Archaean craton to the north of the mobile belt. The area is covered by GGU's geological map at 1:500 000 scale, map sheet 1 'South Greenland' (Allaart, 1975). The map sheet description by Kalsbeek et al. (1990) includes abundant literature references to the geological investigations which were mostly carried out in the western part of South Greenland. An overview of the lithological and structural setting of the Ketilidian mobile belt was given by Allaart (1976). Isotope investigations were published by van Breemen et al. (1974), Patchett & Bridgwater (1984) and Kalsbeek & Taylor (1985), and recently a plate tectonic interpretation of the Ketilidian belt was put forward by Windley (1991).

Allaart (1976) divided the Ketilidian mobile belt into 4 lithotectonic units. From north to south these are: border zone, granite zone, folded migmatite zone and flat-lying migmatite complex (Fig. 1).

The border zone comprises Archaean tonalitic to granodioritic gneisses and basic supracrustal sequences unconformably overlain by Proterozoic metasedimentary and basic metavolcanic rocks. The Proterozoic supracrustals in the border zone are interpreted to represent deposits in a foreland basin (Windley, 1991).

The granite zone is dominated by numerous intrusions of granitoid batholiths with scattered inclusions of supracrustal rocks. An early deformed and metamorphosed group and a later almost non-deformed group of granites have been recognised. Minor plutons of an appinitic (hornblende gabbro) suite are associated with the batholiths. According to isotopic age dating (summarised in Kalsbeek & Taylor, 1985) the granite intrusions were emplaced over a period, c. 1850 to 1740 Ma.

The folded migmatite zone comprises large occurrences of psammitic and pelitic to semipelitic sediments and basic volcanic sequences which are metamorphosed from greenschist up to granulite facies and are migmatised in some areas. The metasediments are intruded by granites of the same general age as those in the granite zone.

The flat-lying migmatite complex consists of flat-lying, high-grade migmatised paragneisses intruded by granitic sheets. The two migmatite zones have undergone strong deformation characterised by thrusting and nappe formation.

A post-tectonic suite of monzonitic to granitic rocks, collectively called rapakivi granites, intrudes both the folded and the flat-lying migmatite zones (Fig. 1).

Isotope studies (van Breemen et al., 1974; Patchett & Bridgwater, 1984; Kalsbeek & Taylor, 1985) gave evidence for very minor involvement of Archaean crustal material in the Ketilidian granites from the granite and the migmatite zones. Accordingly, it is believed that most of the Ketilidian belt represents accretion of new Proterozoic crust onto the Archaean craton.

The Gardar province comprises mid-Proterozoic sediments and lavas deposited in a continental rift zone as well as 10 major alkaline intrusive complexes and numerous dykes emplaced between c. 1300 and 1120 Ma. The latest review of the province is given by Upton & Emeleus (1987).

The geology of the east coast of South Greenland is generally less well known than the western part due to difficult access and terrain. However, the zones defined by Allaart (1976) have been largely recognised. The geological reconnaissance by the Suprasyd programme also sustained this general division, but it is evident that more investigations are needed to solve questions concerning the origin and depositional environment of the supracrustal sequences of the migmatite complex. Also the relationships between the folded migmatite zone and the granite zone need to be studied closer.

Windley (1991) compared the Ketilidian orogen with the Himalayas and suggested that the granite zone represents an Andean-type batholith possibly incorporating earlier accreted mature island arc volcanic and plutonic rocks. He regarded the migmatite zones as belonging to a completely different terrane which was deformed as result of continent-continent collision. The rapakivi suite was suggested to be a product of melting of crustal rocks within a thrust-thickened Tibetan-style plateau, that had begun to undergo extensional collapse. If this continent collision model is correct the southern convergent (Archaean) continent should be sought outside Greenland.

Previous geochemical mapping in South Greenland

Regional sampling of stream sediment and water in South Greenland was undertaken as part of the Sydurán uranium exploration project carried out by GGU in collaboration with Risø National Laboratory (Armour-Brown et al., 1982). About 2300 sites were sampled with an average density of 1 sample per 6 km². The stream sediments were first analysed for 17 major and trace elements and later reanalysed for 34 trace elements.

The first geochemical maps (Armour-Brown et al., 1982; Armour-Brown & Olesen, 1984)) and the later analyses (Steenfelt & Tukiainen, 1990) showed that many element distribution patterns could be related to the litho-tectonic zones and provinces whereas others indicated mineralising events. The boundary between the Archaean craton and the granite province was clearly outlined by the geochemistry and the same was true for the boundary between

the granite province and the folded migmatite zone (Table 3). However, a chemical distinction between the two migmatite zones could not be made, and for this reason the two zones will be collectively termed the migmatite complex in the following.

The Gardar province in general and each of the major intrusive complexes are clearly outlined in the geochemical maps (Table 3; Steenfelt, 1991).

A main result of the Sydurán project was that a large province embracing the majority of the granite zone (including the Gardar igneous province) and migmatite complex was recognised as a geochemical uranium province (Steenfelt & Armour-Brown, 1988) containing several types of uranium mineralisation. The source of the uranium was believed to be the Proterozoic sediments from where uranium has been mobilised and redeposited in veins (Armour-Brown, 1986; Nyegaard & Armour-Brown, 1986).

Another interesting result of the previous geochemical mapping with implications for the economic mineral potential concerned gold (Au) and the gold pathfinder elements arsenic (As) and antimony (Sb) (Steenfelt, 1990; Steenfelt & Tukiainen, 1991). The migmatite complex is characterised by elevated background level for As, several districts with high Sb concentrations and many Au anomalies (Au concentration >20 ppb). In the granite zone a number of Au anomalies occur where the background for As and Sb is low. The granite zone is generally low in As, whereas Sb enrichment is seen in its northern part.

Steenfelt & Tukiainen (1991) stressed the potential for gold mineralisation in the migmatite complex, and particularly in districts where high As, Sb and Au coincide. In fact, a gold bearing quartz vein with Au concentrations in the range of 2 to 235 ppm was found in such a district north of Nanortalik by Nunaoil A/S during field work in 1992 (Nunaoil A/S, press release, Nov. 1992). The find upgrades the potential for similar and other types of gold mineralisation in the migmatite complex.

Physiography

The topography of the surveyed area is rugged and mountainous. The inner Lindenow Fjord is alpine with peaks rising to 2300 m

a.s.l. Along the outer coasts the relief is more moderate. The drainage is mostly supplied by the glaciers and the margins of the inland ice and local ice caps. Apart from local moraines the exposure is excellent. There is very little vegetation. The area is uninhabited and difficult of access.

The airport at Narsarsuaq (see Fig. 1) has connection to Nuuk, the capital of Greenland, and to Iceland, as well as local helicopter services to towns and settlements in South Greenland.

Sampling and analysis

Seven working days were spent sampling 142 sites distributed over a total of c. 10 000 km² of which c. 3000 km² is ice-free area. The sampling of stream sediment and water was combined with gravity measurements at each of the sample sites.

The sample sites were selected and marked on air photos prior to the sampling. It was attempted to get as even a coverage as possible in the difficult and irregular terrain.

At each site c. 500 g of stream sediment was collected in a paper bag and 100 ml of water in a polyethylene bottle. In addition the radioactivity (total gamma-radiation) was measured on the surface of outcrops or stream boulders using a scintillometer (Table 1). Each stream sediment sample was composed of subsamples from 3 to 6 different sand and silt deposits at the stream bed or banks, thus ensuring representative sampling. Duplicate samples of both sediment and water were collected at 4 sites.

Sample preparation and analysis

Sediment. The sample bags were dried at the base camp and then sent by ship to GGU, Copenhagen. Here, the samples were further dried at 65° C and sieved into three grain size fractions using sieve apertures of 1 mm and 0.1 mm. The coarse fraction was discarded, the medium fraction archived, and the fine fraction submitted for analysis to Activation Laboratories Ltd., Canada. The samples were analysed by instrumental neutron activation (INA) method for Au and 34 other elements, by X-ray fluorescence using pressed powder pellets for 14 trace elements (XRF-trace) and by X-ray fluorescence on fused discs, using Li-borate, for major

elements (XRF-major). Some samples did not contain sufficient amounts of the fine fraction to permit all three types of analysis, and this explains the decreasing number of samples analysed: 145 INA, 140 XRF-trace and 132 XRF-major.

Water. The water samples were sent by ship to GGU, Copenhagen, where they were analysed c. 2 months after collection. The conductivity and fluoride concentration were measured.

Data presentation

The analytical results are shown in this report as element distribution maps at the scale of 1:1 000 000 together with summary statistical parameters and histograms of the frequency distribution for each element (Figs 3 to 47). Elements with insignificant concentrations are not included. In cases where an element has been determined by more than one method only one of the data sets is presented: the one regarded as the most reliable or determined at the lowest detection limit.

In the element distribution maps the size of a dot is proportional to the concentration in the sample. The scaling of the dot size is chosen so that regional variations in the geochemical background are displayed as clearly as possible. Maximum values are found in the statistical parameters in the figures, and values regarded as geochemical anomalies are shown on the anomaly maps (Figs 48 and 49).

Comments on the element distribution patterns

Geochemical variation related to crustal structure

Despite the relatively small number of samples collected, particularly in the northern part of the survey area, geochemical provinces are clearly outlined which reflect the major lithotectonic units, the granite zone, and the migmatite complex, Table 4. The Archaean craton is only represented by 4 or 5 samples and, therefore, the boundary to the granite zone is not so well established. However, the boundary defined by decrease in Ni, Cr and Sc (Figs 30, 19 and 34) south of Puisortoq agrees with the position of the boundary as judged by geological observations

during the Suprasyd field work (Nielsen et al. in review), but disagrees slightly with the boundary of Allaart (see Fig. 1).

The southern boundary of the granite zone, marked by a decrease of a number of elements (Table 4), follows the fjord Avarqat Kangerluat (see Fig. 2), and again the geochemical boundary disagrees only slightly with the suggested litho-tectonic boundary. On the north shore of the northern branch of Avarqat Kangerluat there are anomalies in Nb, Ga and Zn (Fig. 48 and 49), and also high values of Rb (Fig. 32) and F (in water; Fig. 47). This association is characteristic of the Gardar syenites and it is possible that the anomalies are caused by Gardar dykes. The stream sediment results do not otherwise indicate an extension of the Gardar province to the east coast.

The geochemical province with high concentrations of As and other elements listed in Table 4 has a northern limit almost along 61°N, i.e. south of the geological boundary between the migmatite complex and the granite province. The high values appear to be located in regions where supracrustal rocks predominate (over synorogenic granite and rapakivi granites). This situation is analogue to western South Greenland where the As province also has its boundary c. 20 km southeast of the boundary against the granite province. Windley (1991) suggested that the boundary between the granite zone and the migmatite complex is a major shear zone, although this has not been documented in the field. Further interpretation of the relationship between the geochemical and lithological or structural features must await additional field work.

Indications of mineralisation

Gold. The distribution of Au, As, Sb (Figs 14, 13, 34) shows that the province with potential for gold mineralisation recognised in the western part of South Greenland (Steenfelt & Tukiainen, 1990) continues to the east coast. Anomalies of these elements cluster around Dænells Fjord and outer Lindenow Fjord (Fig. 48). These areas are dominated by supracrustal rocks, psammitic and pelitic metasediments with intercalations of basic metavolcanics, which are migmatised and intruded by granites. This

setting is very reminiscent of the regional setting at the gold mineralisation north of Nanortalik, but more investigations of the supracrustal sequences in the migmatite complex are needed to establish how these may be correlated.

Uranium. The mean uranium concentration over the survey area is 34 ppm, which is very high compared to average crustal values, 2.8 ppm in the upper crust (Taylor & McLennan, 1985). The mean for the rest of South Greenland was also 34 ppm (Olesen, 1984), and it is evident that the South Greenland geochemical uranium province (Armour-Brown et al., 1983; Steenfelt & Armour-Brown, 1988) extends to the east coast.

Tungsten. In the geochemical surveys based on the fine fraction of stream sediment over most of Greenland the concentration of W is below the detection limit. The high W values in the southern migmatite complex is, therefore, considered suggestive of W mineralisation. However, the significance of the W concentration cannot be evaluated properly before the source of the W has been identified.

Copper, lead and zinc. There are a few high values of these metals scattered over the survey area with some clustering of Cu and Zn in the migmatite complex. None of the values are very high, but they may be worth following-up, as conspicuous rust zones, observed during the Suprasyd reconnaissance, suggest that sulphide mineralisation has taken place in the supracrustals.

Thorium, niobium and hafnium. The stream sediments derived from rapakivi granites are known from the Sydurán geochemical mapping to be characterised by very high concentrations of Zr, Y, Nb, Th and Hf (Olesen, 1984 and unpublished data). Accordingly, most of the anomalies for these elements (Fig. 49) occur within or close to mapped occurrences of rapakivi granites (compare with Fig. 2).

Conclusion

The reconnaissance geochemical survey of a section of the east coast of South Greenland showed that litho-tectonic units and geochemical provinces recognised in the western part of South Greenland continue in the eastern part. An exception is the prominent Gardar alkaline igneous province which seems to be

largely restricted to western South Greenland. The geochemical anomaly pattern indicates that the Proterozoic metasedimentary and subordinate metavolcanic rocks around Danell Fjord and Lindenow Fjord have a potential for gold and uranium mineralisation.

References

- Allaart, J.H. 1975: Geological map of Greenland. 1:500 000 sheet 1, Sydgrønland. Copenhagen: Geol. Surv. Greenland.
- Allaart, J.H. 1976: Ketilidian mobile belt in South Greenland. In Escher, A. & Watt, W.S. (edit.) *Geology of Greenland*, 121-151. Copenhagen: Geol. Surv. Greenland.
- Armour-Brown, A. 1986: Geology and evaluation of the uranium mineral occurrence at Igdlorssuit, South Greenland. Unpubl. report, Geol. Surv. Greenland, 60 pp.
- Armour-Brown, A. & Olesen, B.L. 1984: Condensing multi-element reconnaissance geochemical data from South Greenland using empirical discriminant analysis. *J. geochem. Explor.* 21, 395-404.
- Armour-Brown, A., Tukiainen, T. & Wallin, B. 1982: The South Greenland uranium exploration programme. Final report. Unpubl. report, Geol. Surv. Greenland, 95 pp.
- Kalsbeek, F., Larsen, L.M. & Bondam, J. 1990: Descriptive text to 1:500 000 sheet 1, Sydgrønland. Copenhagen: Geol. Surv. Greenland, 36 pp.
- Kalsbeek, F. & Taylor, P.N. 1985: Isotopic and chemical variation in granites across a Proterozoic continental margin - the Ketilidian mobile belt of South Greenland. *Earth Planet. Sci. Lett.* 73, 65-80.
- Nielsen, T.F.D. et al. in review: Suprasyd 1992, South Greenland. *Rapp. Grønlands geol. Unders.*
- Nyegaard, P.N. & Armour-Brown, A. 1986: Uranium occurrences in the granite zone. Structural setting - genesis - exploration methods. Unpubl. report, Geol. Surv. Greenland, 138 pp.
- Olesen, B.L. 1984: Geochemical mapping of South Greenland. Unpubl. thesis, Dept Mineral Industry, Technical Univ. Denmark, 132 pp.
- Patchett, P.J. & Bridgwater, D. 1984: Origin of the continental crust of 1.9 - 1.7 Ga age defined by Nd isotopes in the Ketilidian terrain of South Greenland. *Contr. Miner. Petrol.* 87, 311-318.

- Steenfelt, A. 1990: Gold content of regional stream sediment samples from South Greenland. *Open File Ser. Grønlands geol. Unders.* 90/5, 12 pp.
- Steenfelt, A. 1991: High-technology metals in alkaline and carbonatitic rocks in Greenland: recognition and exploration. *J. geochem. Explor.* 40, 263-279.
- Steenfelt, A. & Armour-Brown, A. 1988: Characteristics of the South Greenland uranium province. In IAEA (ed.) *Recognition of uranium provinces*, 305-335. Vienna: International Atomic Energy Agency.
- Steenfelt, A. & Tukiainen, T. 1991: Geochemical mapping: distribution of gold, antimony and tantalum in South Greenland. *Rapp. Grønlands geol. Unders.* 152, 55-61.
- Upton, B.G.J. & Emeleus, C.H. 1987: Mid-Proterozoic alkaline magmatism in South Greenland: The Gardar Province. In Fitton, J.G. & Upton, B.G.J. (edit.) *Alkaline Igneous Rocks*. Geol. Soc. London, Spec. Publ., 30, 449-471.
- van Breemen, O., Aftalion, M. & Allaart, J.H. 1974: Isotopic and geochronologic studies on granites from the Ketilidian mobile belt of South Greenland. *Bull. geol. Soc. Amer.* 85, 403-412.
- Windley, B.F. 1991: Early Proterozoic collision tectonics, and rapakivi granites as intrusions in an extensional thrust-thickened crust: the Ketilidian orogen, South Greenland. *Tectonophysics* 195, 1-10.

Table 1. Instrumentation at the Geological Survey of Greenland

Field measurement of gamma-radiation: Saphymo-Srat SPP-2
scintillometer

Water samples:

Conductivity: Chemotest JK 8800

Fluoride concentration: Orion EA 920 pH/ion analyser

Table 2. Analytical detection limits.

Instrumental Neutron Activation Analysis (Activation Laboratories Ltd.)

Au	5.0 ppm	Ag	5.0 ppm	As	2.0 ppm	Ba	100.0 ppm
Br	1.0 ppm	Ca	1.0 %	Co	5.0 ppm	Cr	10.0 ppm
Cs	2.0 ppm	Fe	0.02 %	Hf	1.0 ppm	Hg	1.0 ppm
Ir	5.0 ppm	Mo	5.0 ppm	Na	500.0 ppm	Ni	50.0 ppm
Rb	30.0 ppm	Sb	0.2 ppm	Sc	0.1 ppm	Se	5.0 ppm
Sn	0.01 %	Sr	0.05 %	Ta	1.0 ppm	Th	0.5 ppm
U	0.05 ppm	W	4.0 ppm	Zn	50.0 ppm	La	1.0 ppm
Ce	3.0 ppm	Nd	5.0 ppm	Sm	0.1 ppm	Eu	0.2 ppm
Tb	0.5 ppm	Yb	0.05 ppm	Lu	0.05 ppm		

X-ray Fluorescence Spectrometry (pressed powder pellets)
(Activation Laboratories Ltd.)

Ba	5.0 ppm	Co	5.0 ppm	Cr	5.0 ppm	Cu	5.0 ppm
Ga	5.0 ppm	Nb	2.0 ppm	Ni	5.0 ppm	Pb	5.0 ppm
Rb	2.0 ppm	Sr	2.0 ppm	V	5.0 ppm	Y	2.0 ppm
Zn	5.0 ppm	Zr	5.0 ppm				

Table 3. Stream sediment geochemical characteristics of lithotectonic units in **western** South Greenland; based on Armour-Brown et al. (1982), Olesen (1984), Steenfelt & Tukiainen (1990).

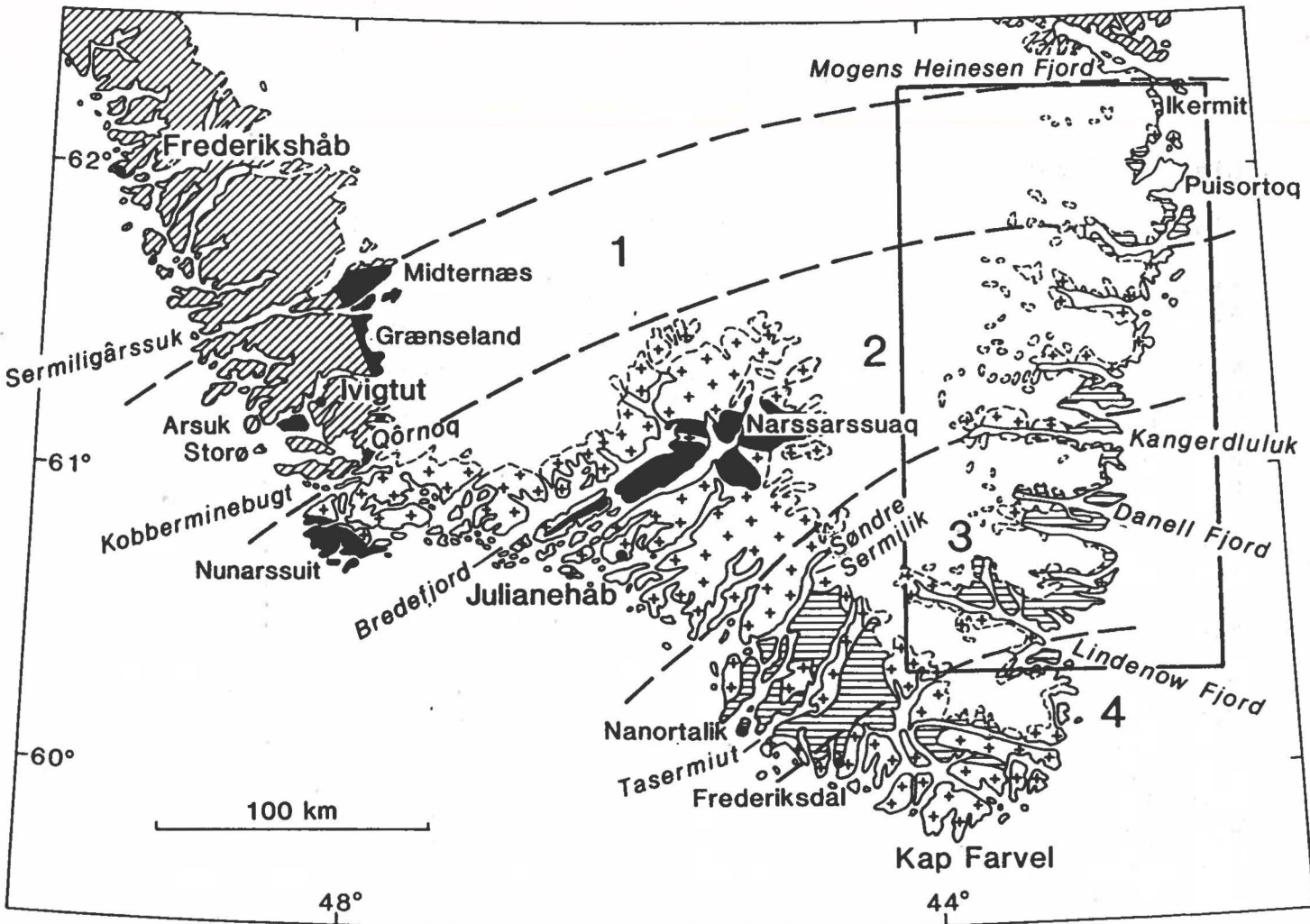
	High concentration	Low concentration
Archaean and border zone:	Ni,Cr	K,Rb,U,Y,Zr
Granite zone:	Sr,U	Rb,Zn
Migmatite complex:	K,Rb,U,Zr,As	Sr
Gardar province:	Ga,Nb,Ta,Zn,Rb,Y,REE	Sr

Table 4. Stream sediment geochemical characteristics of lithotectonic units in **eastern** South Greenland based on the present survey.

	High concentration	Low concentration
Archaean and border zone:	Ni,Cr,Sc	K,Rb,U
Granite zone:	Al,V,Ti,P,Sr,Na,Ba	Cr,Sb,Ni
Migmatite complex south of 61°N:	As,Au,Cs,Rb,Sb, Sm,Th,U,W,Y,Yb	Sr,P,Ba
Gardar?	F,Nb,Zn	

List of figures

- Fig. 1. Location of the survey area in South Greenland.
- Fig. 2. Simplified geological map of the survey area. After Allaart (1976).
- Fig. 3. Geochemical map of: SiO_2 in stream sediment
- Fig. 4. TiO_2
- Fig. 5. Al_2O_3
- Fig. 6. Fe_2O_3
- Fig. 7. MnO
- Fig. 8. MgO
- Fig. 9. CaO
- Fig. 10. Na_2O
- Fig. 11. K_2O
- Fig. 12. P_2O_5
- Fig. 13. As
- Fig. 14. Au
- Fig. 15. Ba
- Fig. 16. Br
- Fig. 17. Ce
- Fig. 18. Co
- Fig. 19. Cr
- Fig. 20. Cs
- Fig. 21. Cu
- Fig. 22. Eu
- Fig. 23. Ga
- Fig. 24. Hf
- Fig. 25. La
- Fig. 26. Lu
- Fig. 27. Mo
- Fig. 28. Nb
- Fig. 29. Nd
- Fig. 30. Ni
- Fig. 31. Pb
- Fig. 32. Rb
- Fig. 33. Sb
- Fig. 34. Sc
- Fig. 35. Sm
- Fig. 36. Sr
- Fig. 37. Th
- Fig. 38. U
- Fig. 39. V
- Fig. 40. W
- Fig. 41. Y
- Fig. 42. Yb
- Fig. 43. Zn
- Fig. 44. Zr
- Fig. 45. Map of gamma-radiation
- Fig. 46. Geochemical map of: Conductivity of stream water.
- Fig. 47. Fluoride
- Fig. 48. Geochemical anomaly map, Au,As,Sb,Cu,Pb,Zn
- Fig. 49. Geochemical anomaly map, U,Th,Nb,Hf,Ga,W

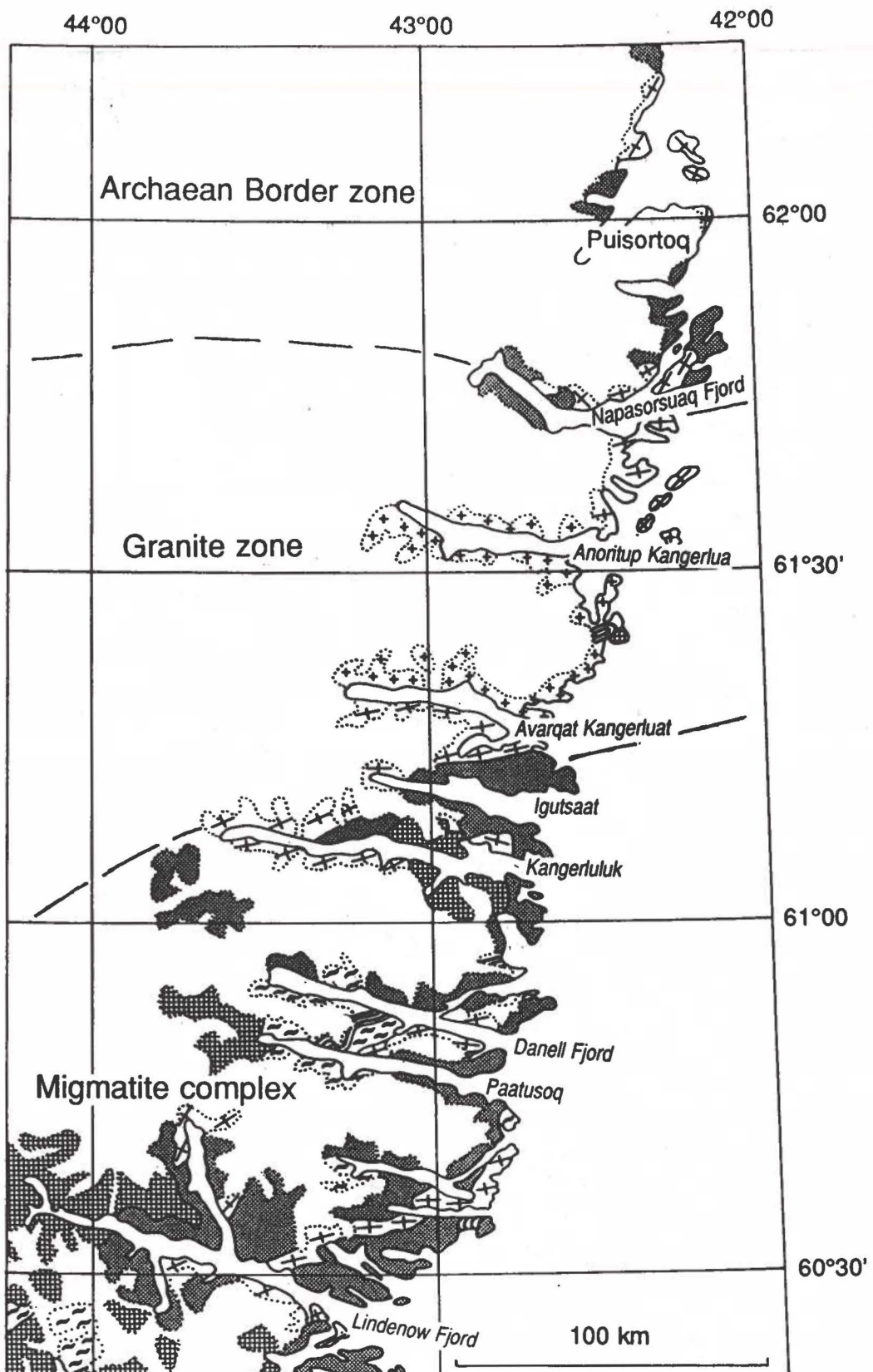


Structural division and main geological units in South Greenland. From Kalsbeek et al. (1990). The survey area is framed.

- Zone 1: northern border zone
- Zone 2: granite zone
- Zone 3: folded migmatite zone
- Zone 4: flat-lying migmatite complex

- syn- and post orogenic granites
- Proterozoic metasediments and metavolcanic rocks
- in zone 1: Proterozoic supracrustals on Archaean basement
- in zone 2: major intrusive complexes of the Gardar province
- Archaean basement

Fig. 1



- | | | | |
|---------------------------|------------------|-----------------------------------|--------------------------|
| [Rapakivi granite symbol] | Rapakivi granite | [Supracrustals symbol] | Supracrustals |
| [Late granite symbol] | Late granite | [Migmatitic metapelite symbol] | Migmatitic metapelite |
| [Early granite symbol] | Early granite | [Basic metavolcanic rocks symbol] | Basic metavolcanic rocks |

Fig. 2

SiO₂ (pct) in stream sediment



X-ray Fluorescence

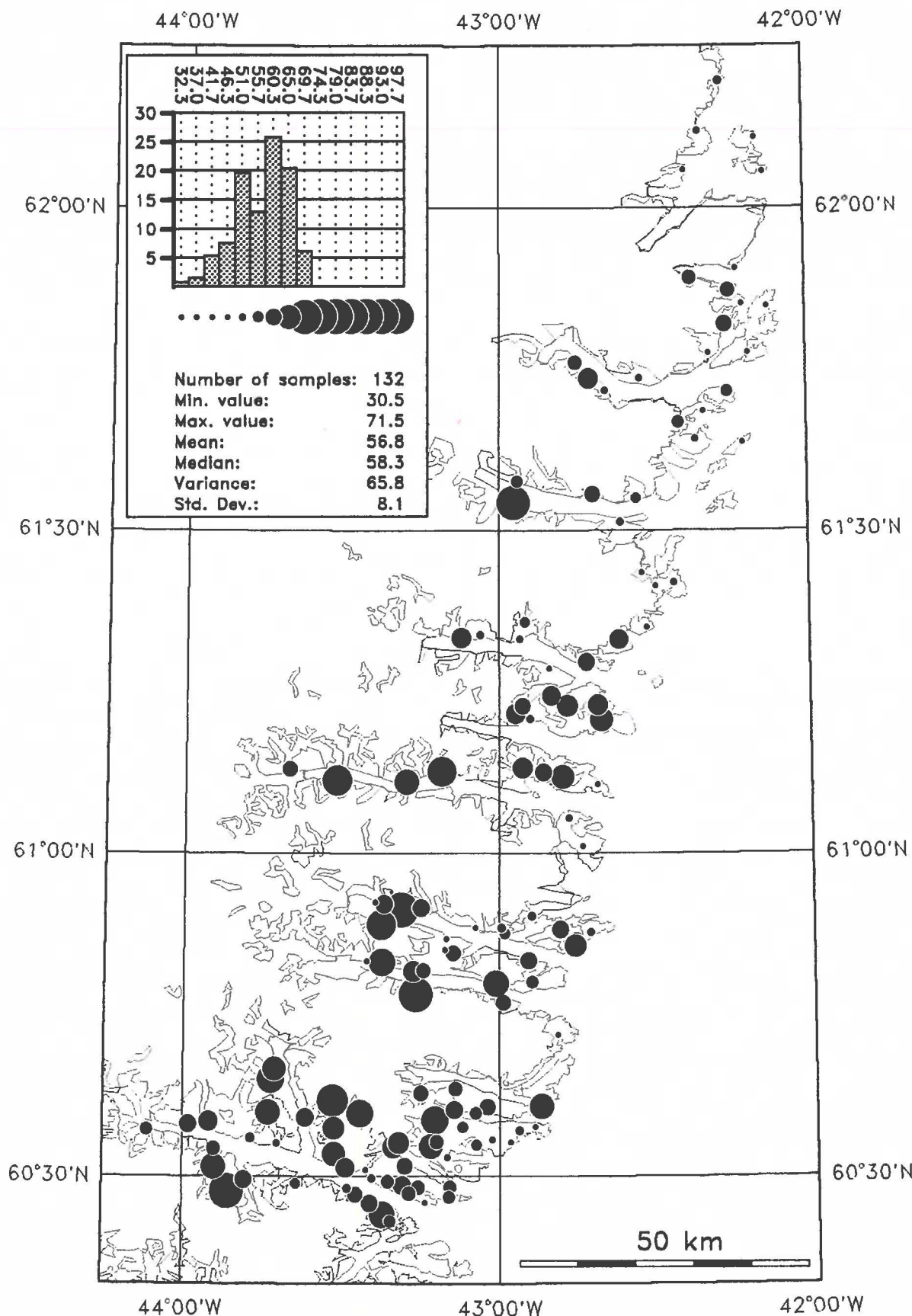


Fig. 3

TiO₂ (pct) in stream sediment



X-ray Fluorescence

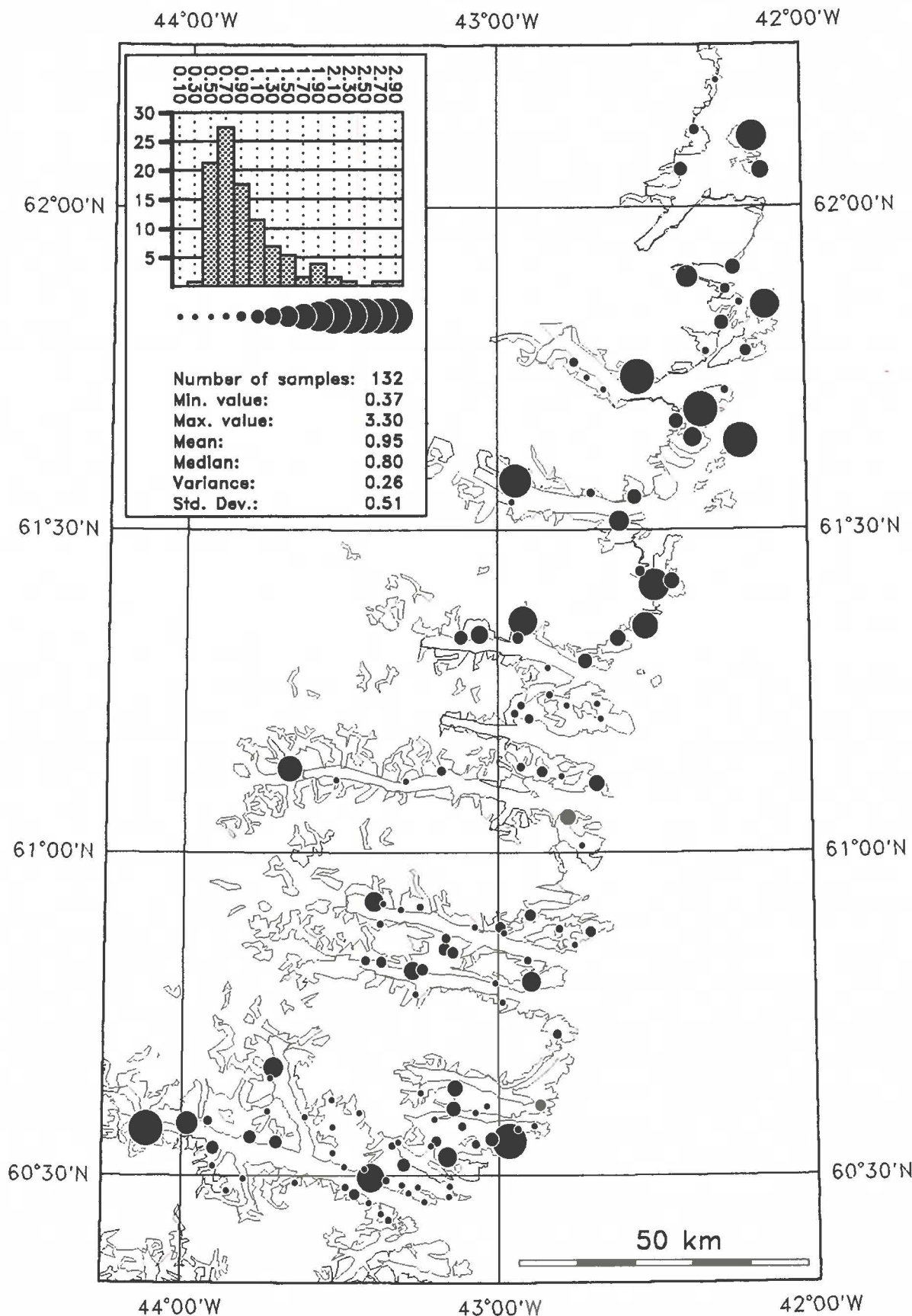


Fig. 4

Al₂O₃ (pct) in stream sediment



X-ray Fluorescence

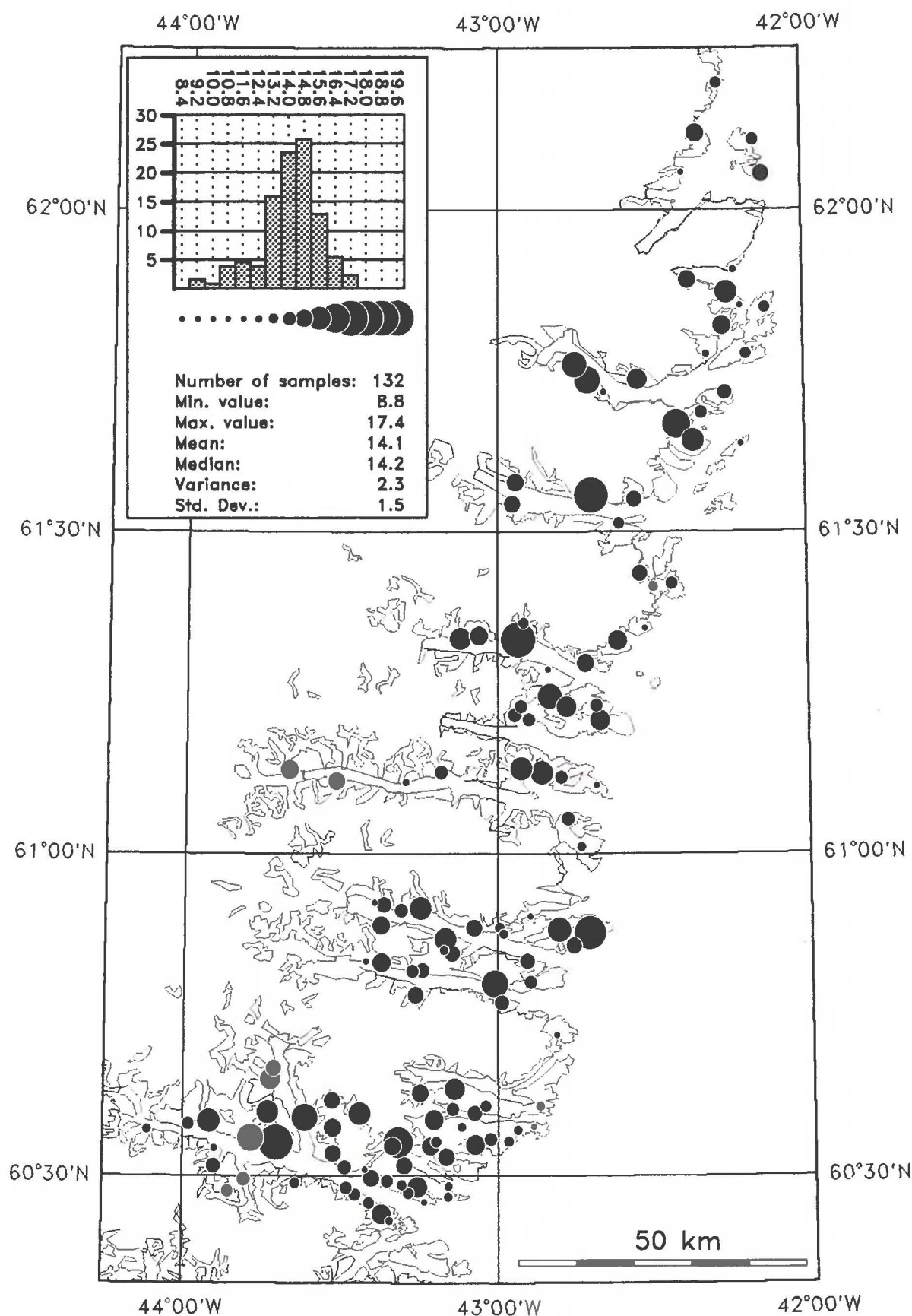


Fig. 5

Fe₂O₃ (pct) in stream sediment



X-ray Fluorescence

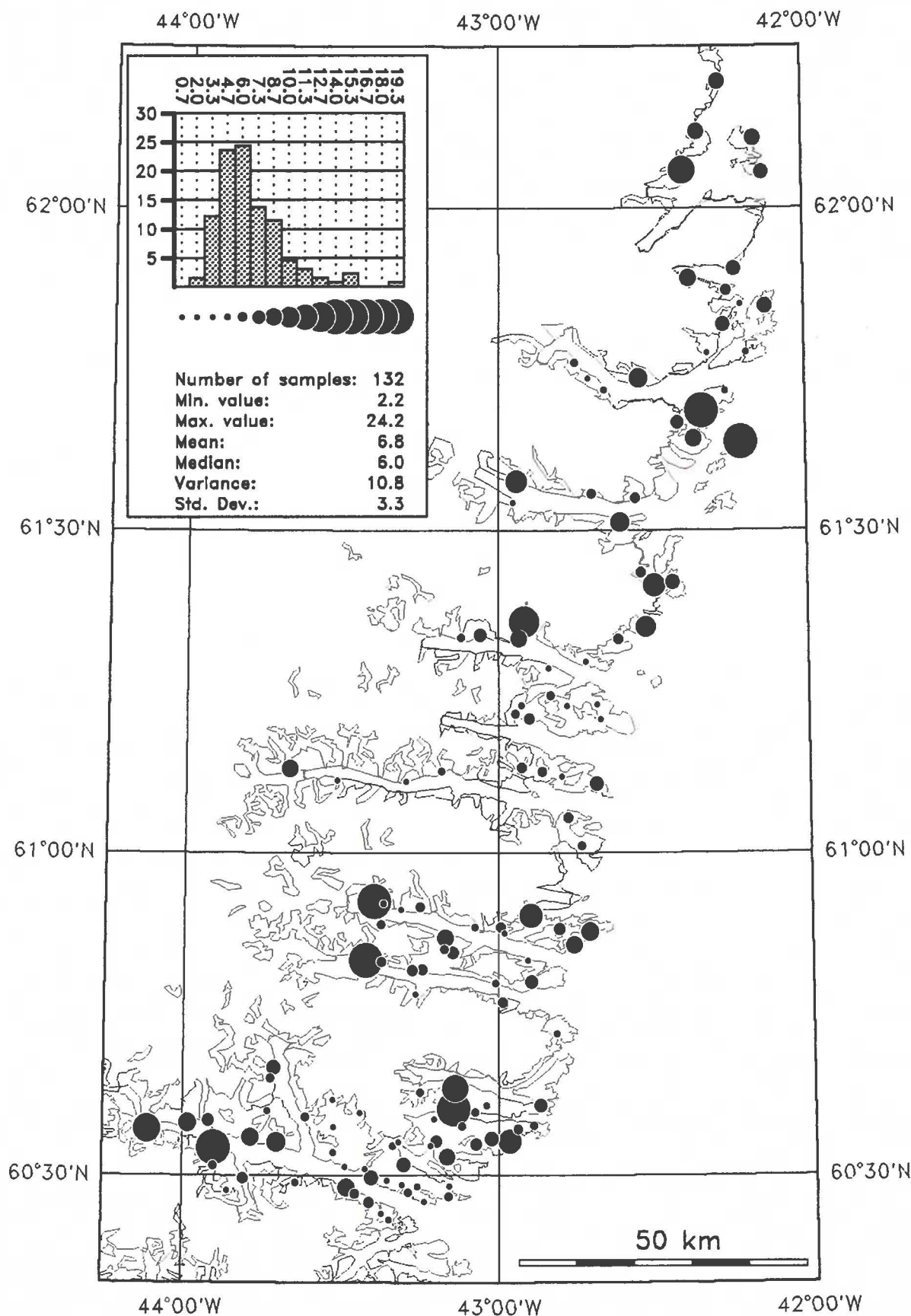


Fig. 6

MnO (pct) in stream sediment



X-ray Fluorescence

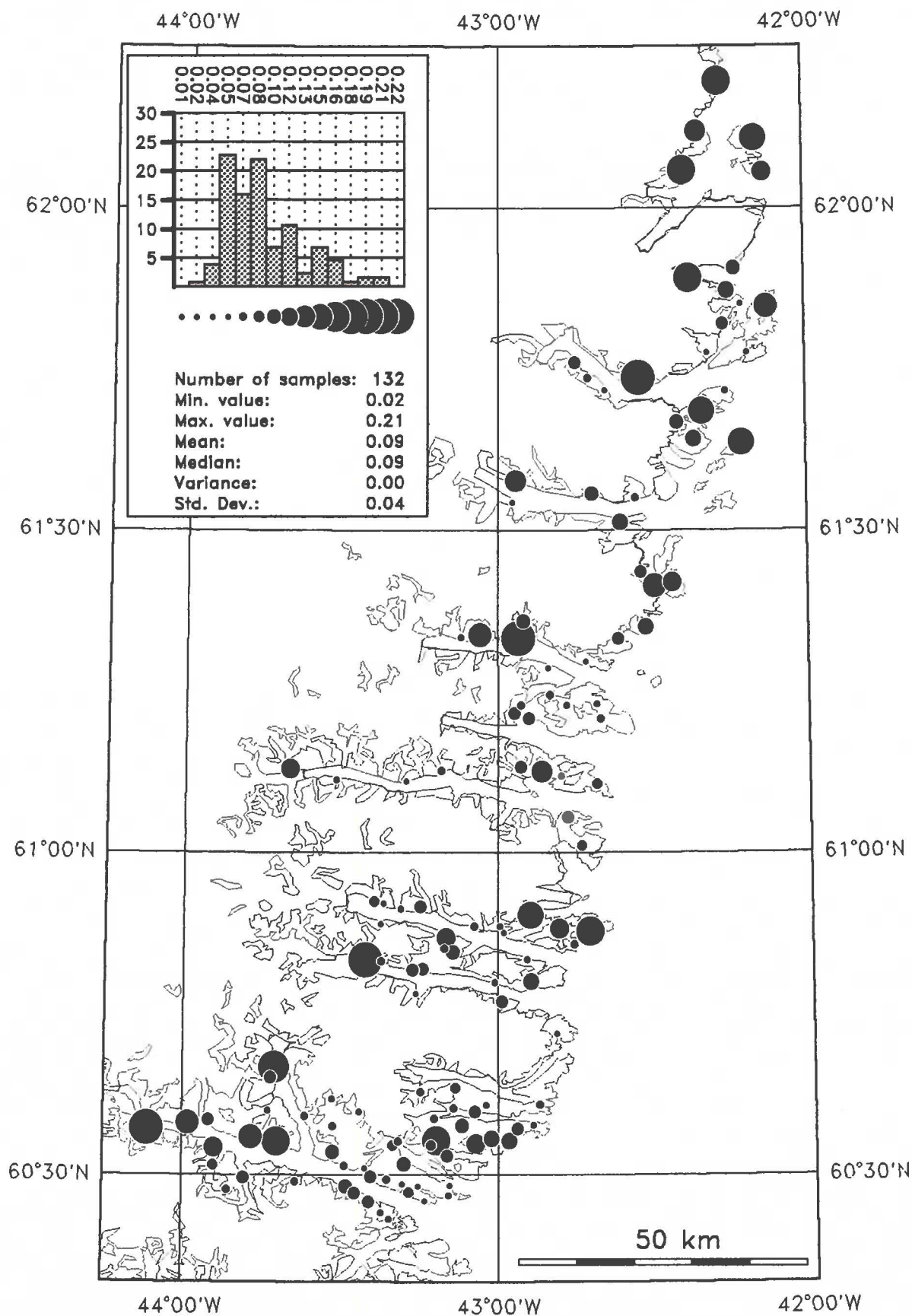


Fig. 7

MgO (pct) in stream sediment



X-ray Fluorescence

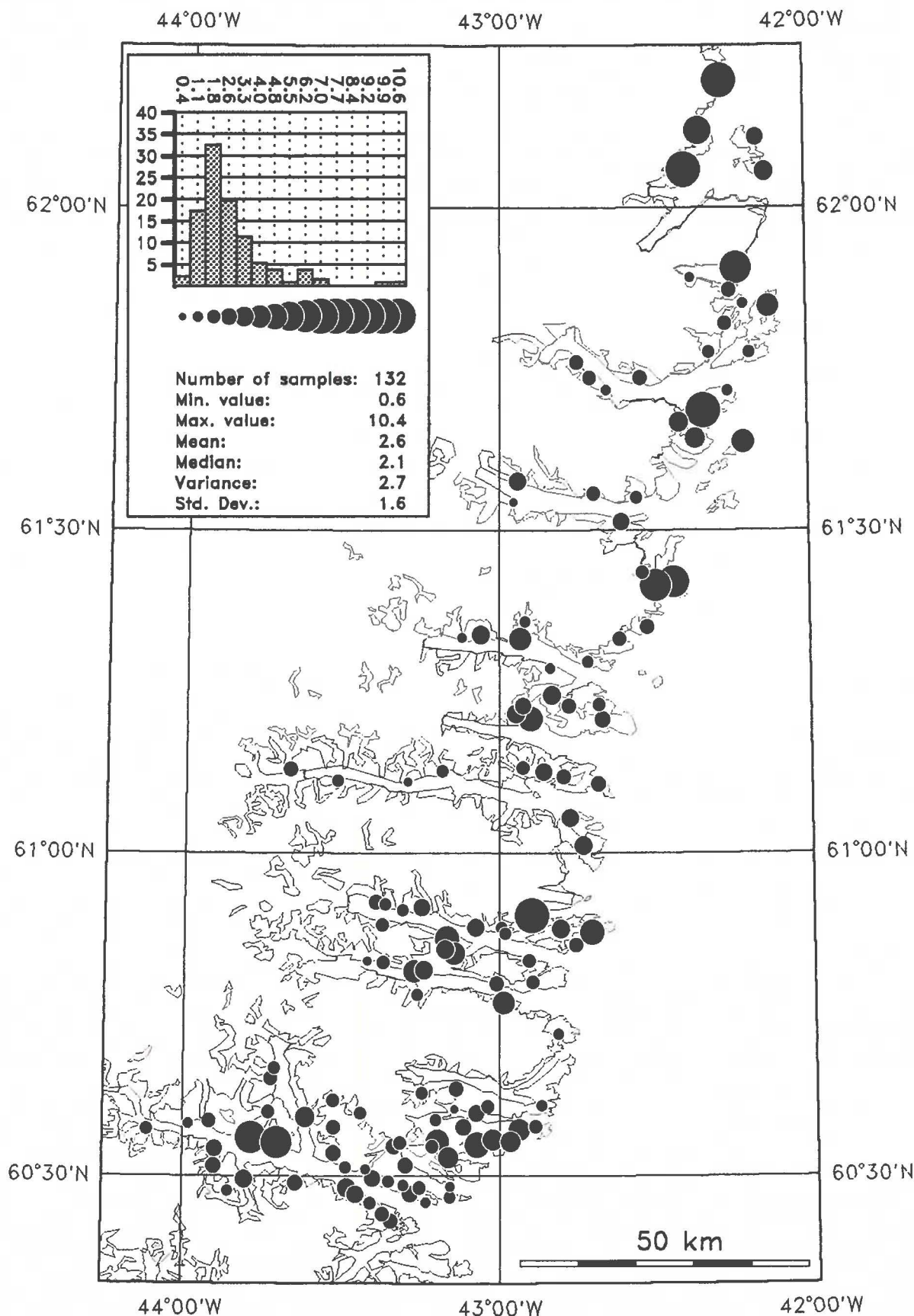


Fig. 8

CaO (pct) in stream sediment



X-ray Fluorescence

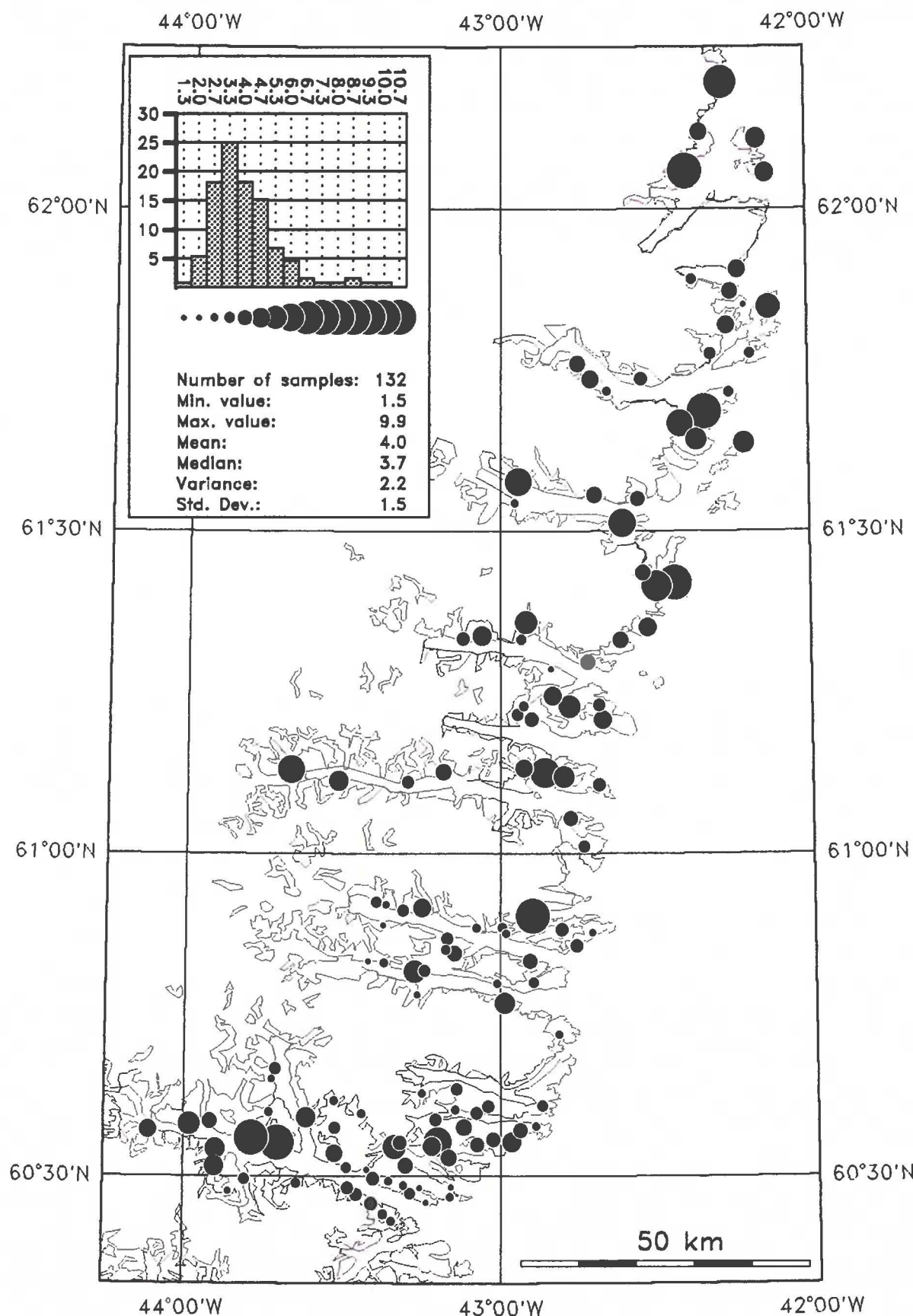


Fig. 9

Na₂O (pct) in stream sediment



X-ray Fluorescence

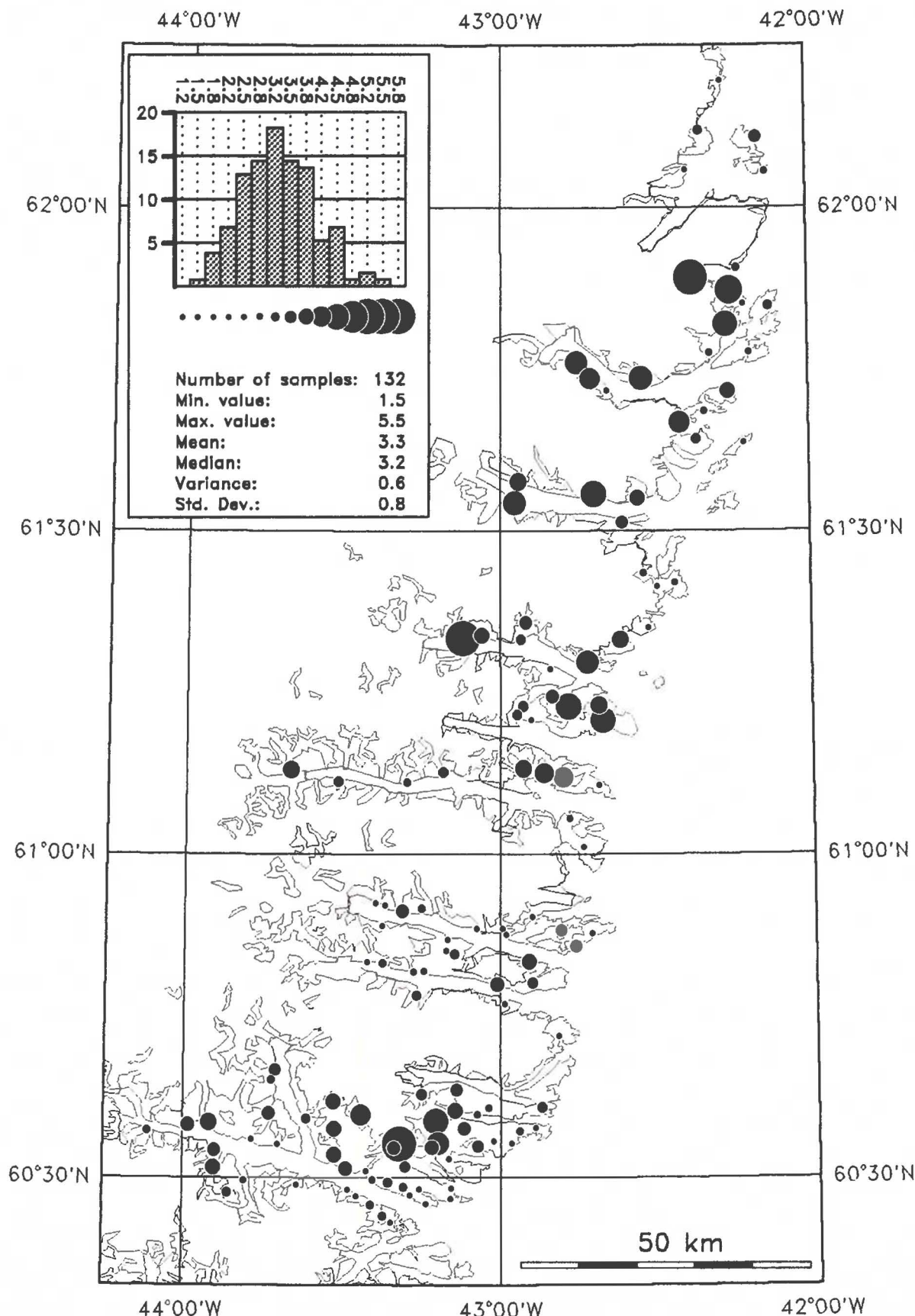


Fig. 10

K2O (pct) in stream sediment



X-ray Fluorescence

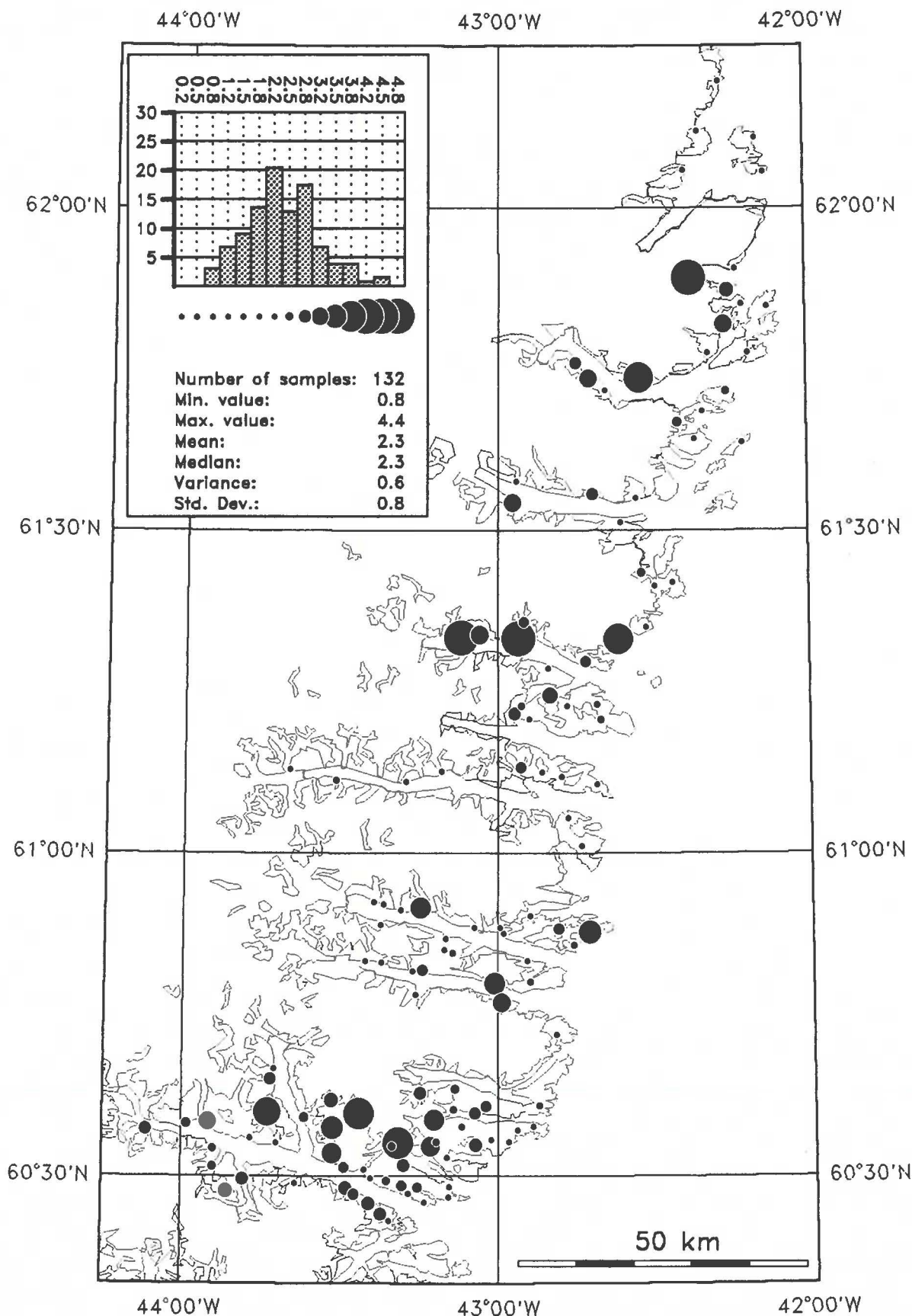


Fig.11

P205 (pct) in stream sediment



X-ray Fluorescence

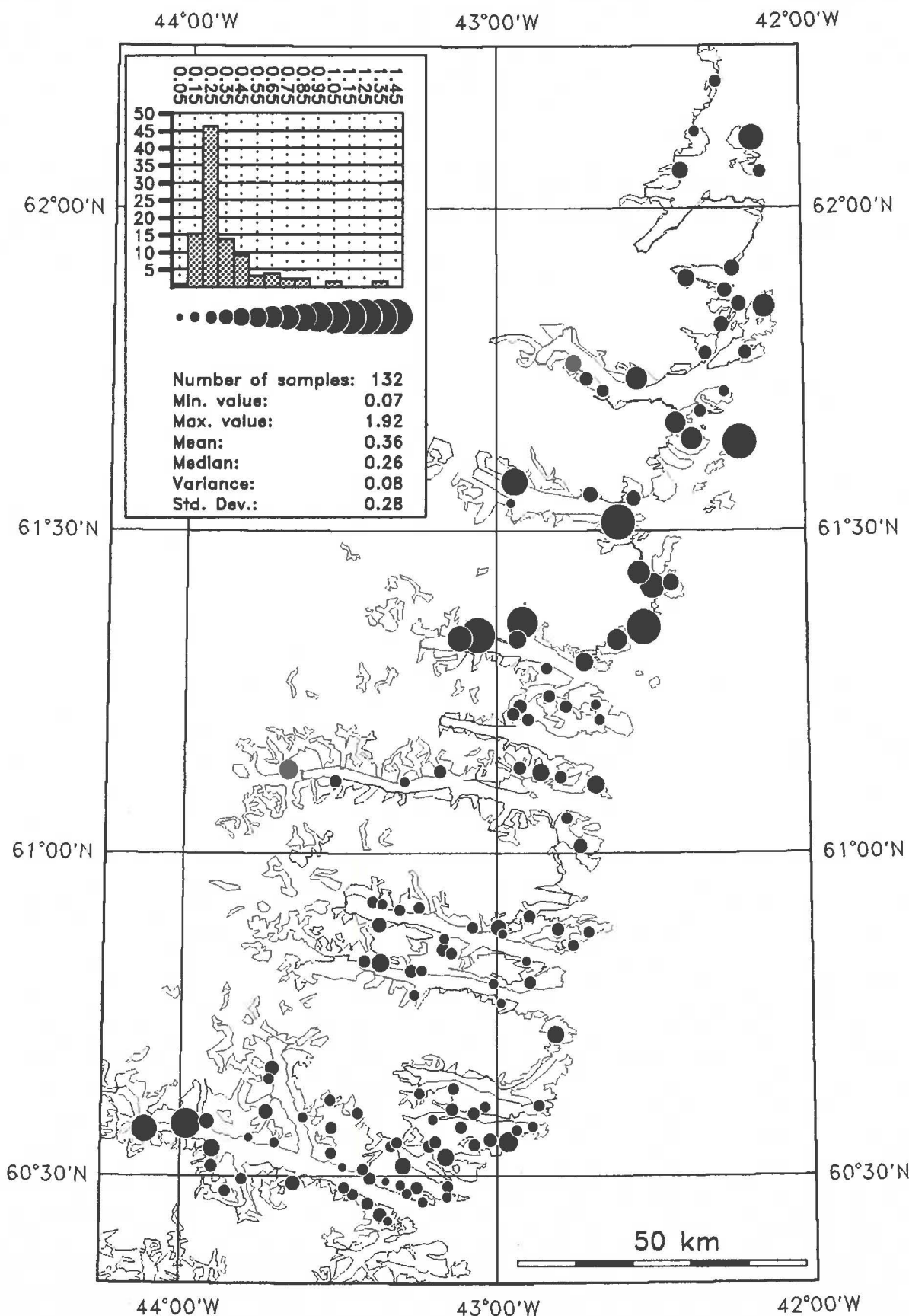


Fig. 12

As (ppm) in stream sediment



Instrumental Neutron Activation

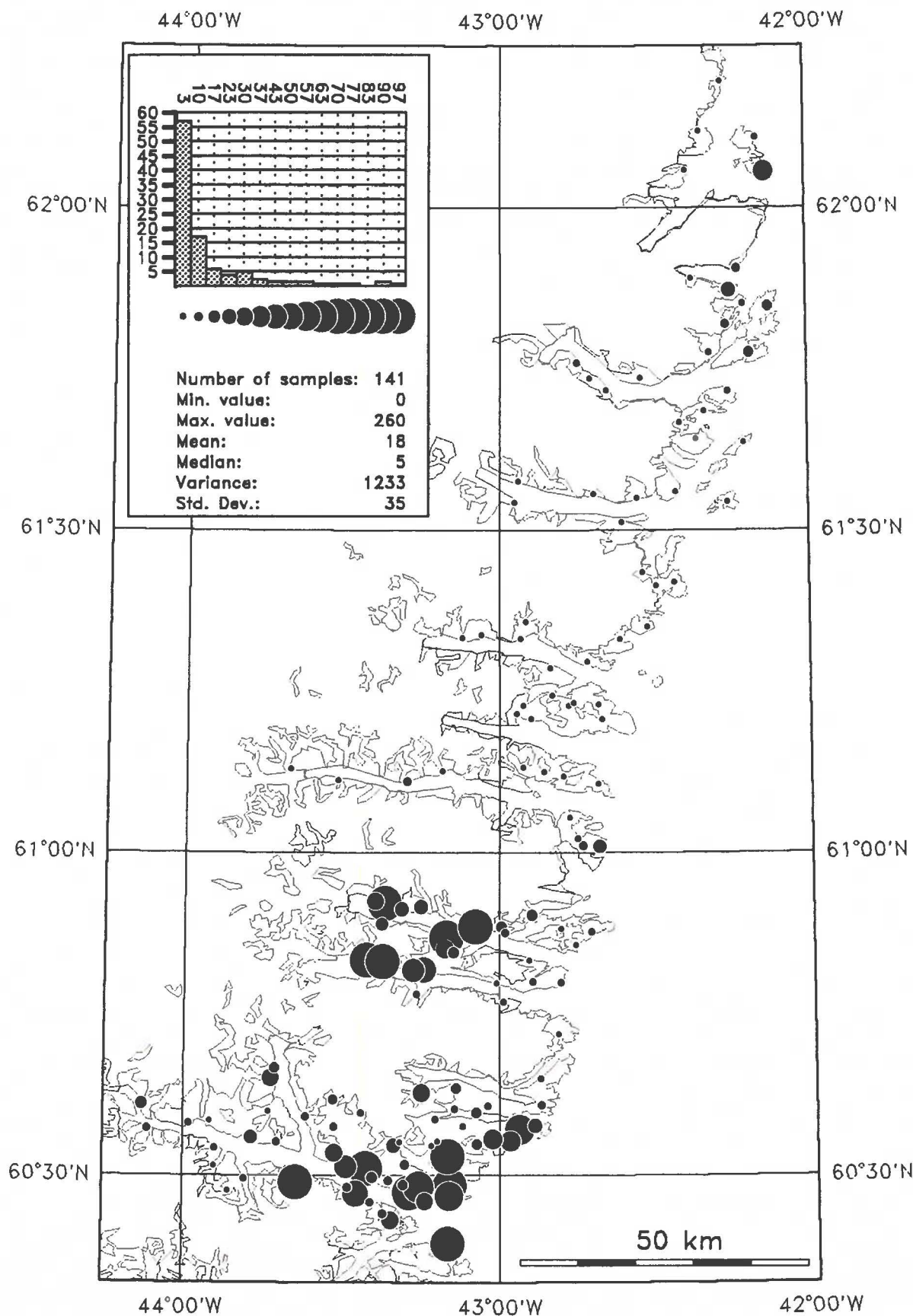


Fig.13

Au (ppb) in stream sediment

Instrumental Neutron Activation

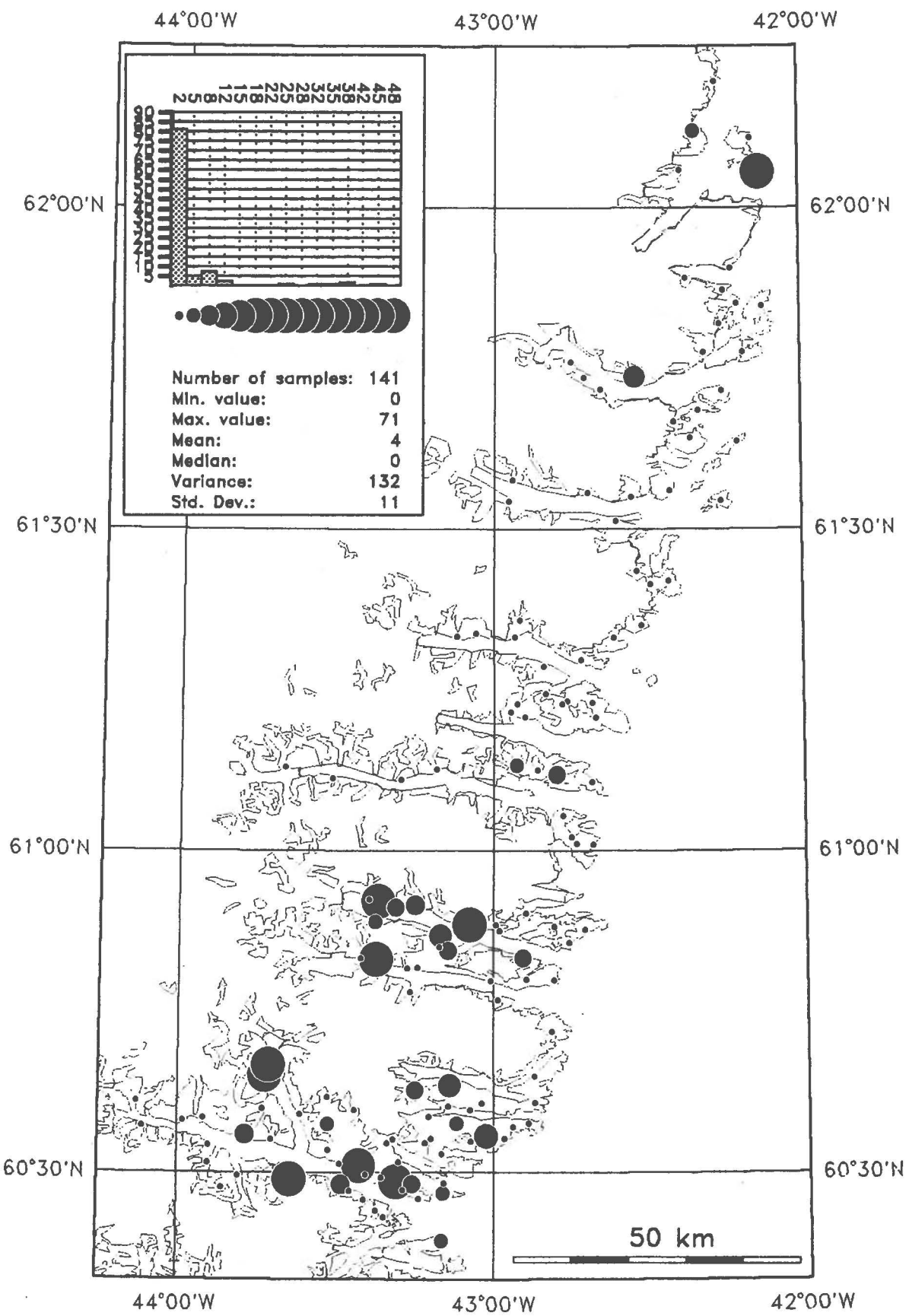


Fig. 14

Ba (ppm) in stream sediment



X-ray Fluorescence

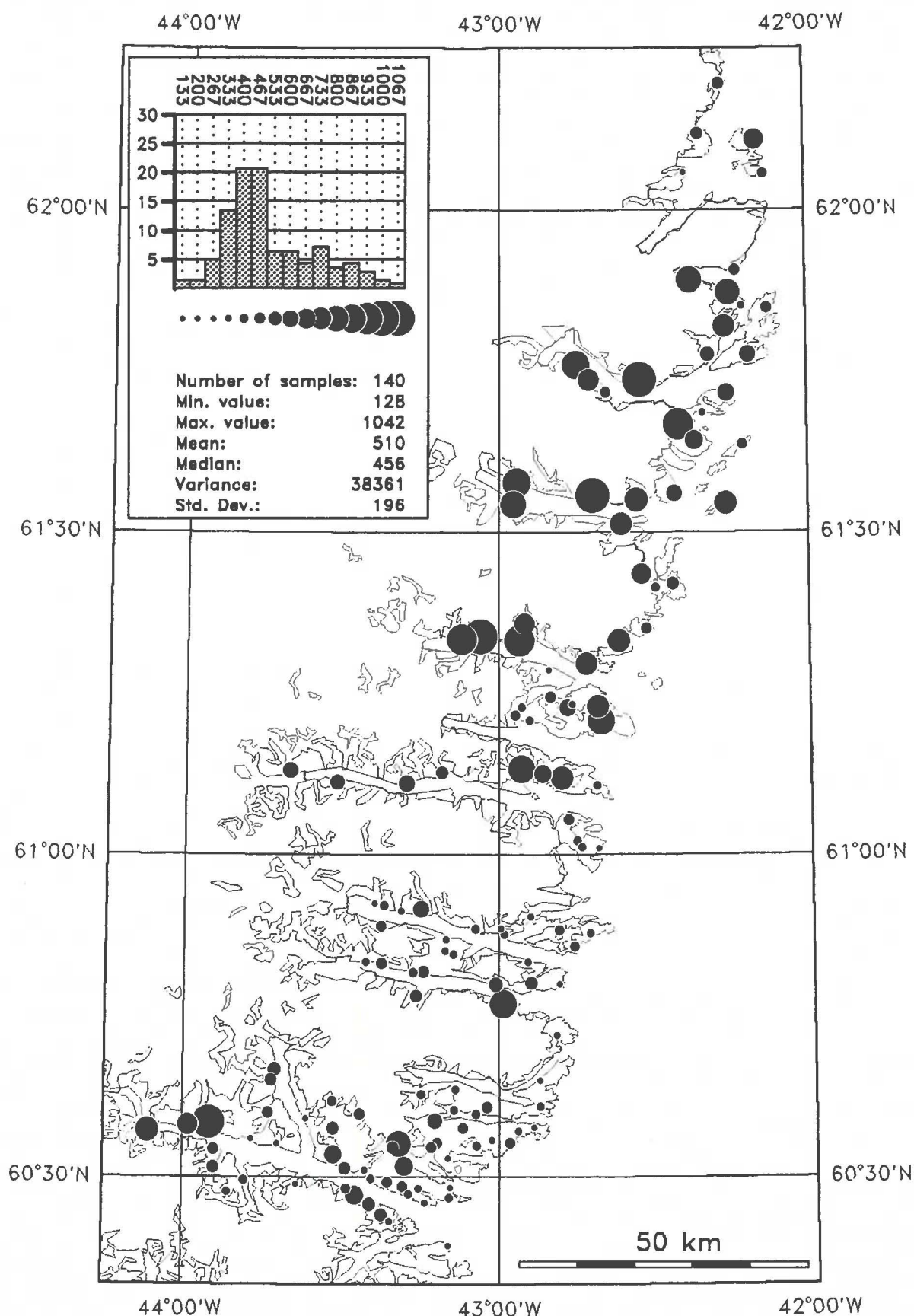


Fig.15

Br (ppm) in stream sediment



Instrumental Neutron Activation

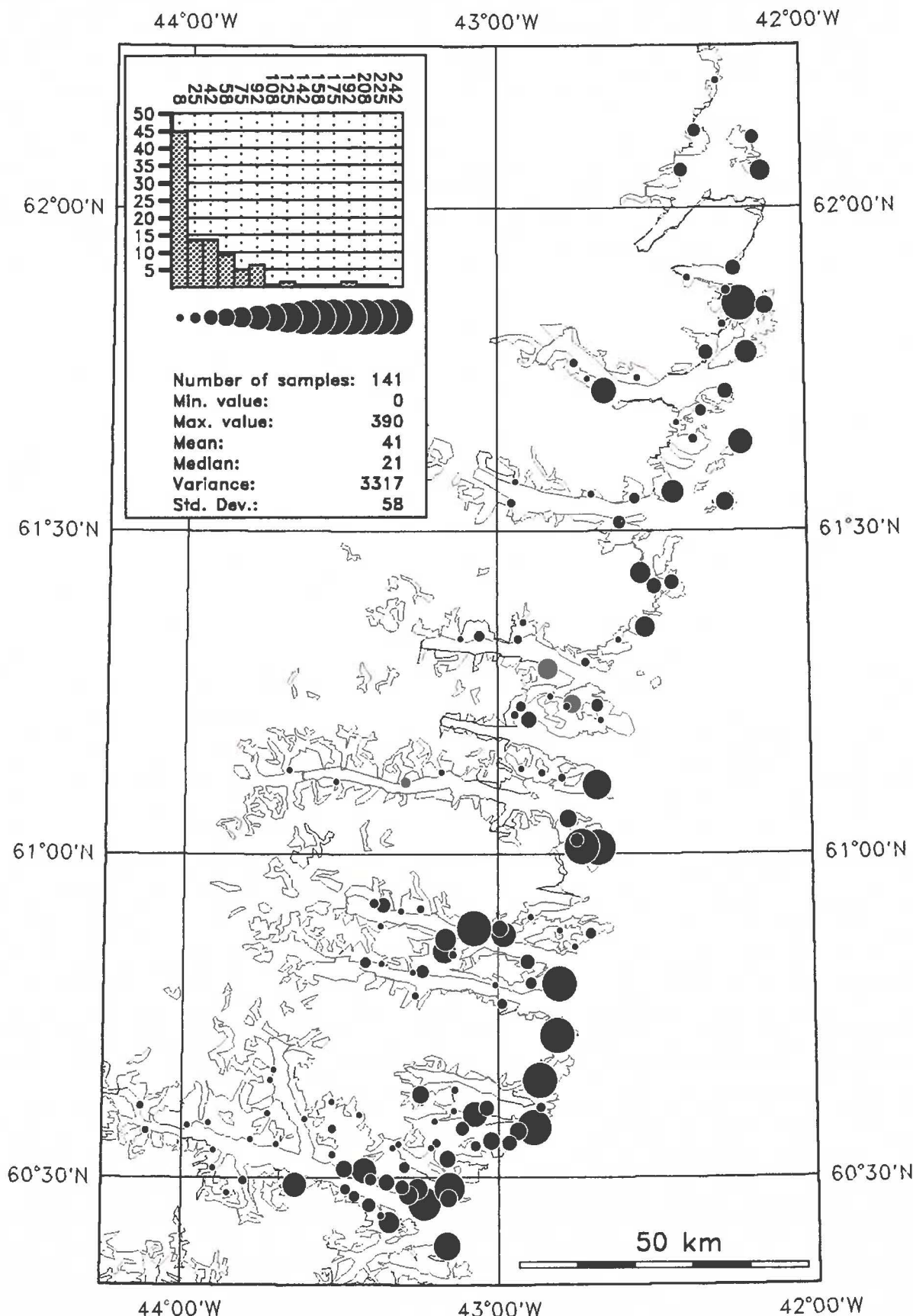


Fig. 16

Ce (ppm) in stream sediment

Instrumental Neutron Activation

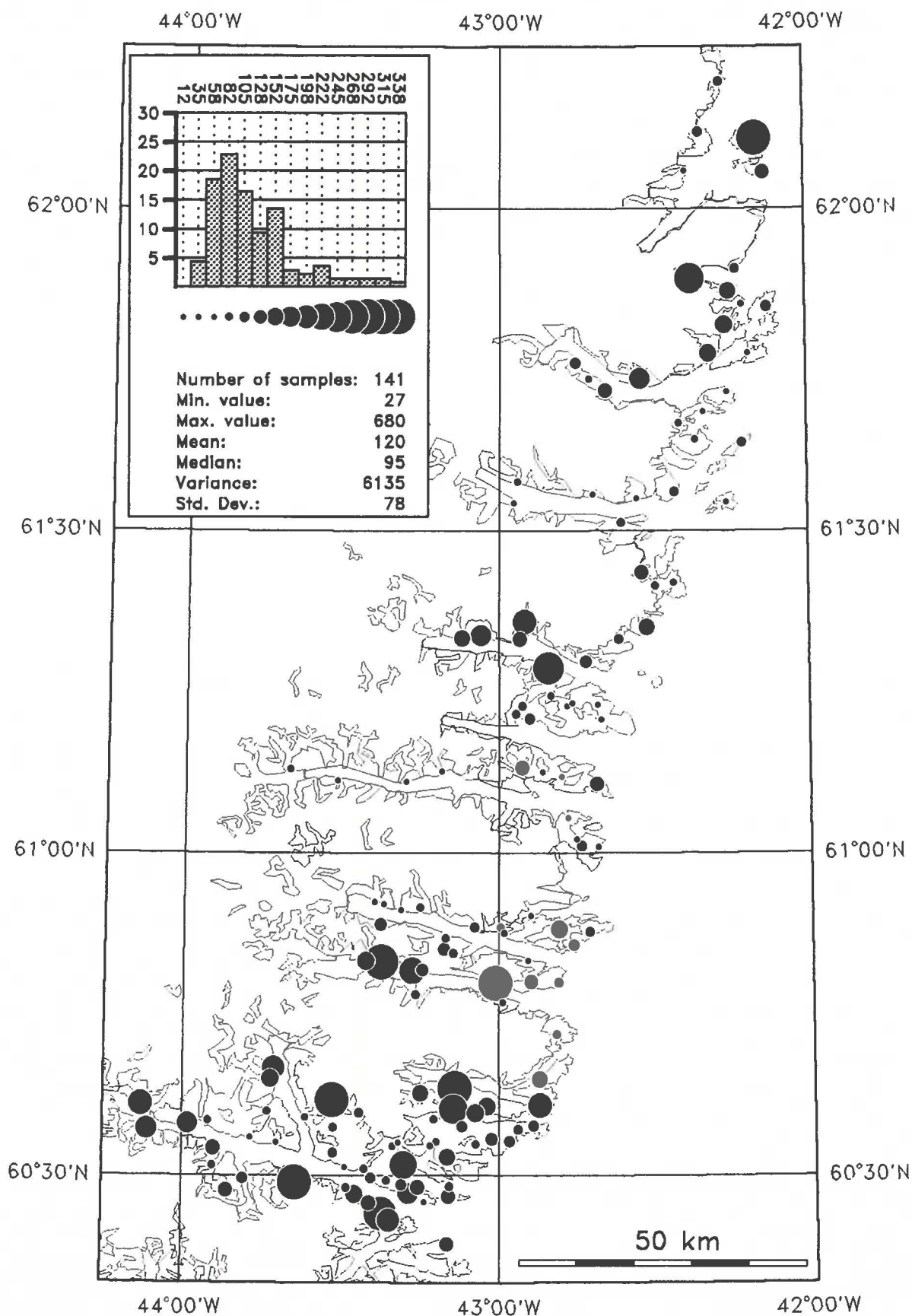


Fig. 17

Co (ppm) in stream sediment



X-ray Fluorescence

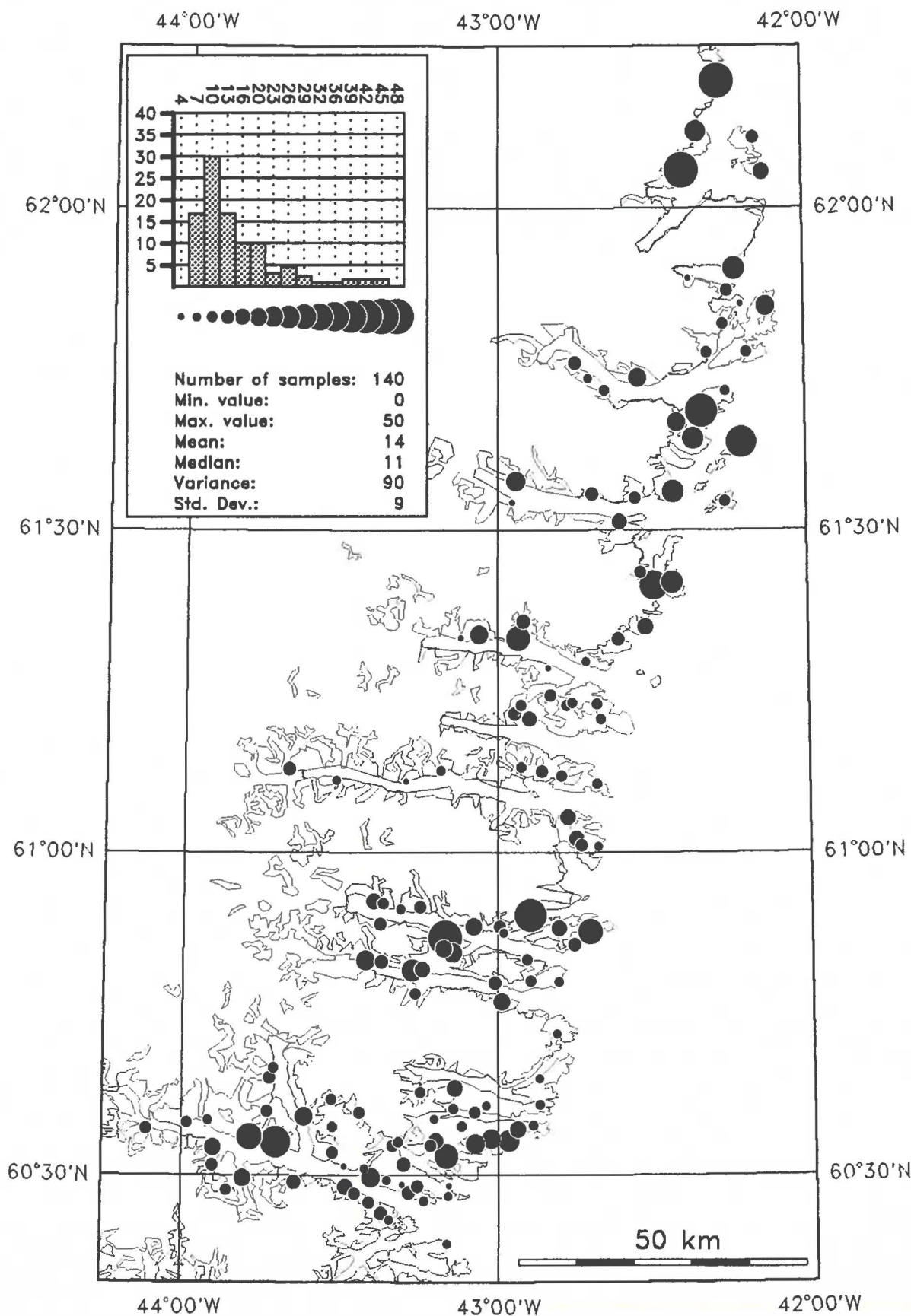


Fig. 18

Cr (ppm) in stream sediment



X-ray Fluorescence

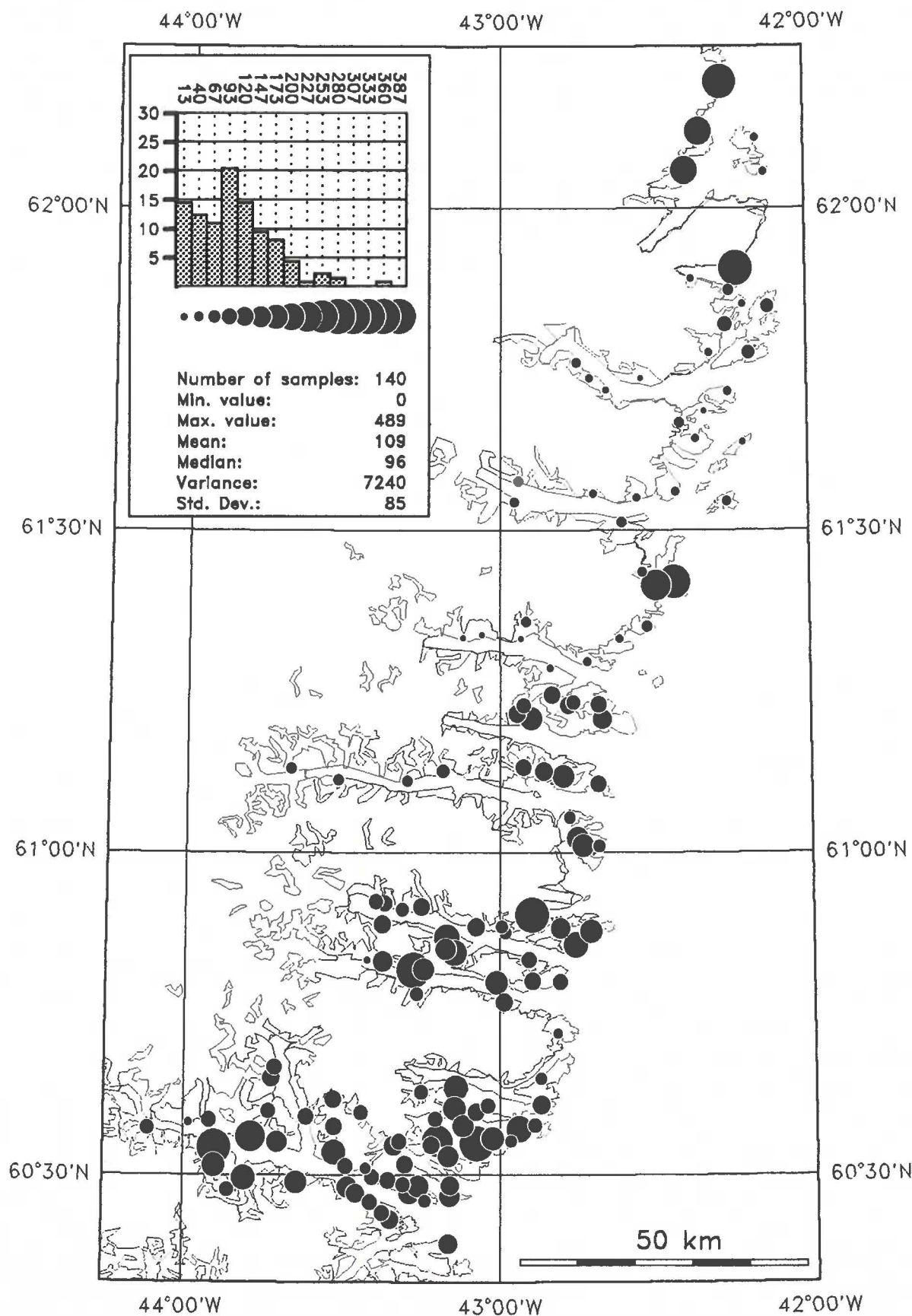


Fig. 19

Cs (ppm) in stream sediment

Instrumental Neutron Activation

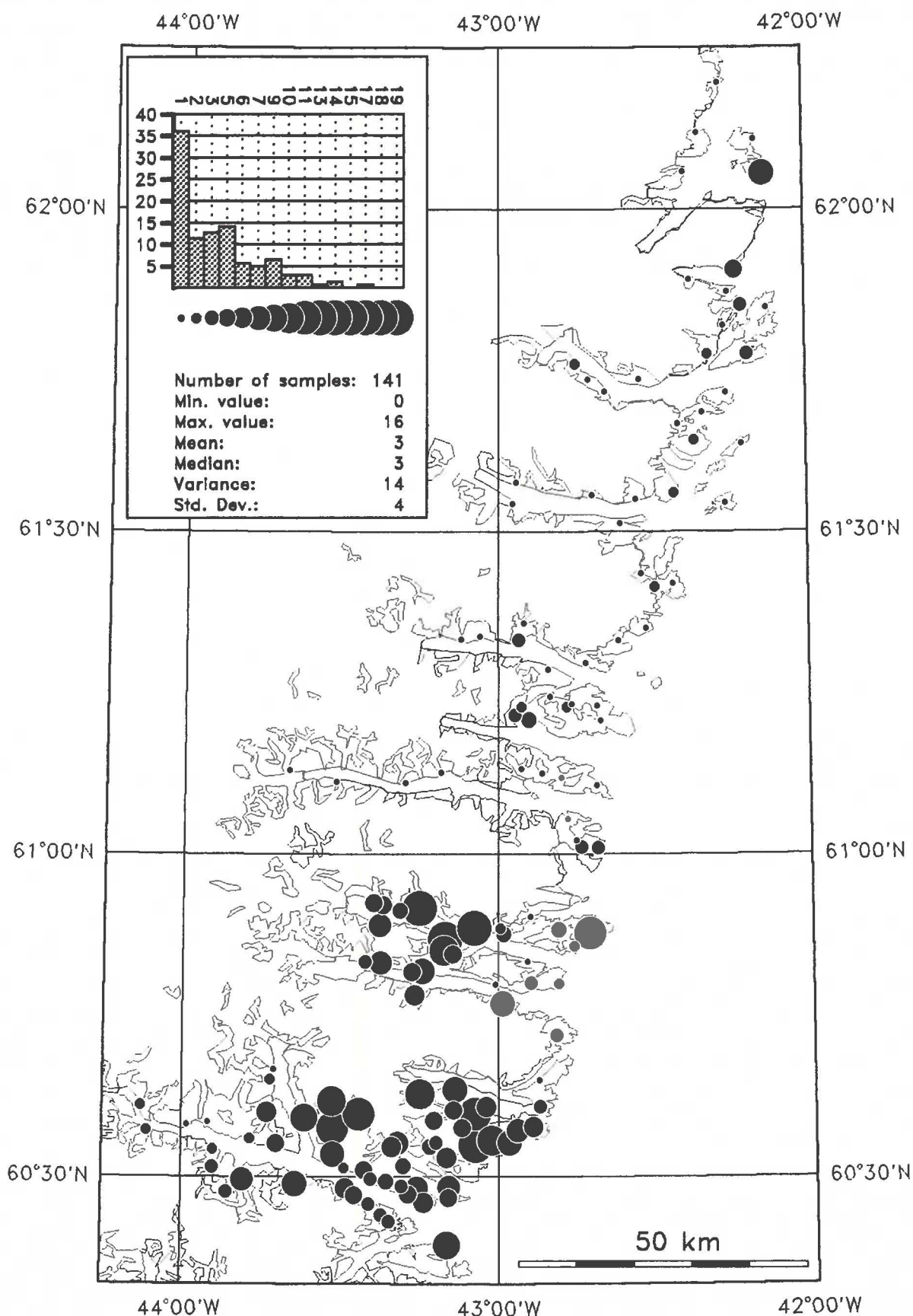


Fig. 20

Cu (ppm) in stream sediment



X-ray Fluorescence

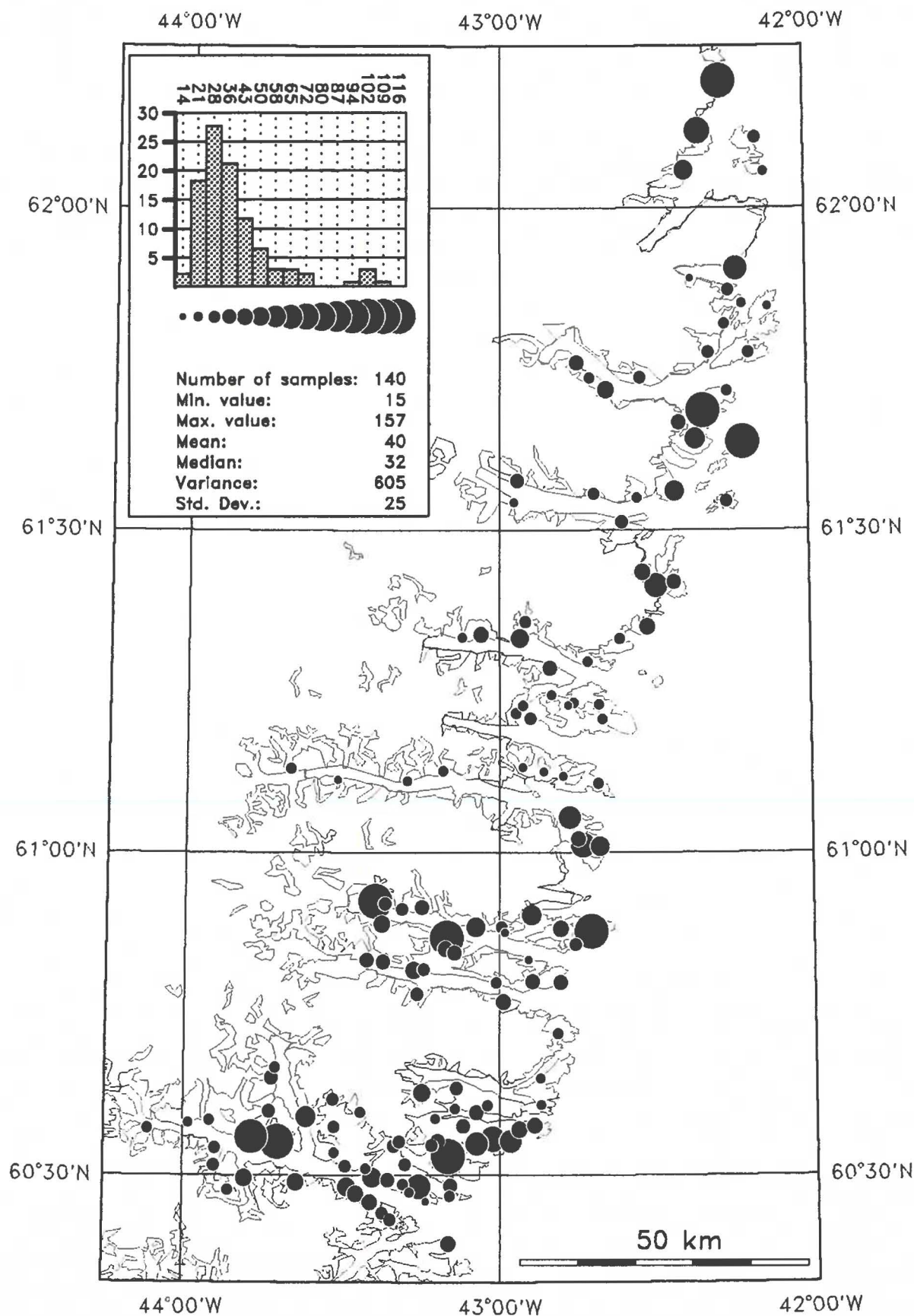


Fig. 21

Eu (ppm) in stream sediment



Instrumental Neutron Activation

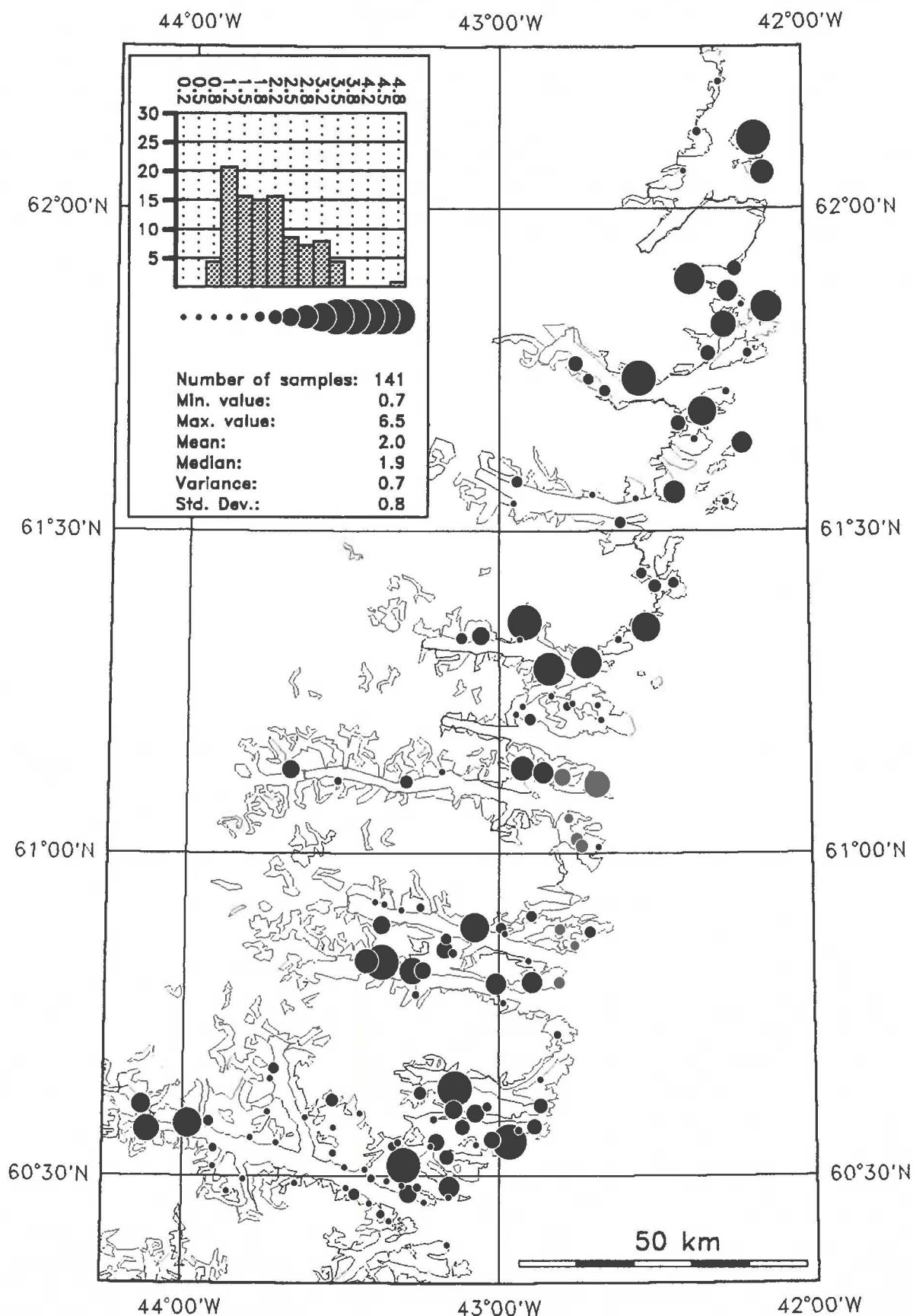


Fig. 22

Ga (ppm) in stream sediment



X-ray Fluorescence

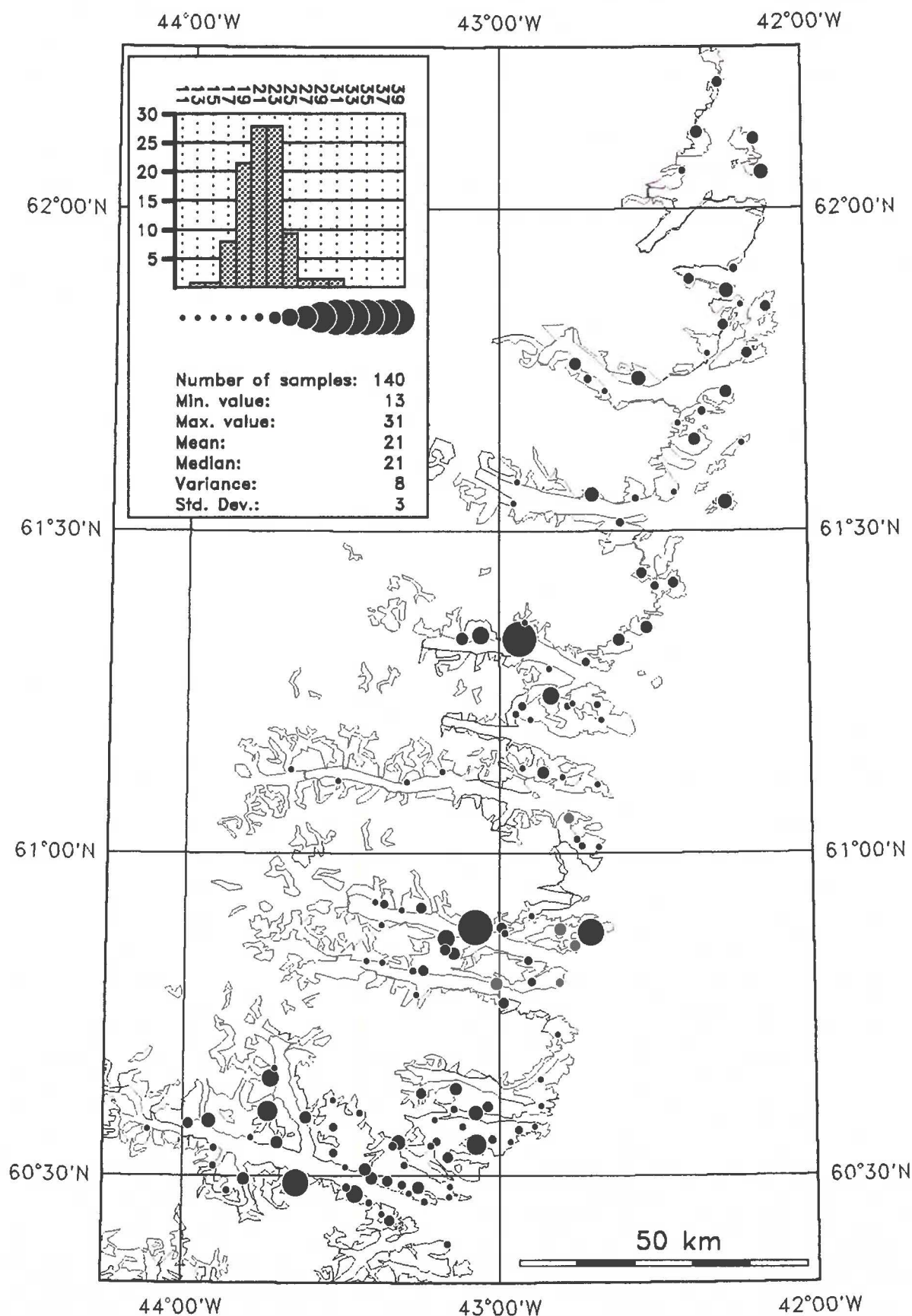


Fig. 23

Hf (ppm) in stream sediment

Instrumental Neutron Activation

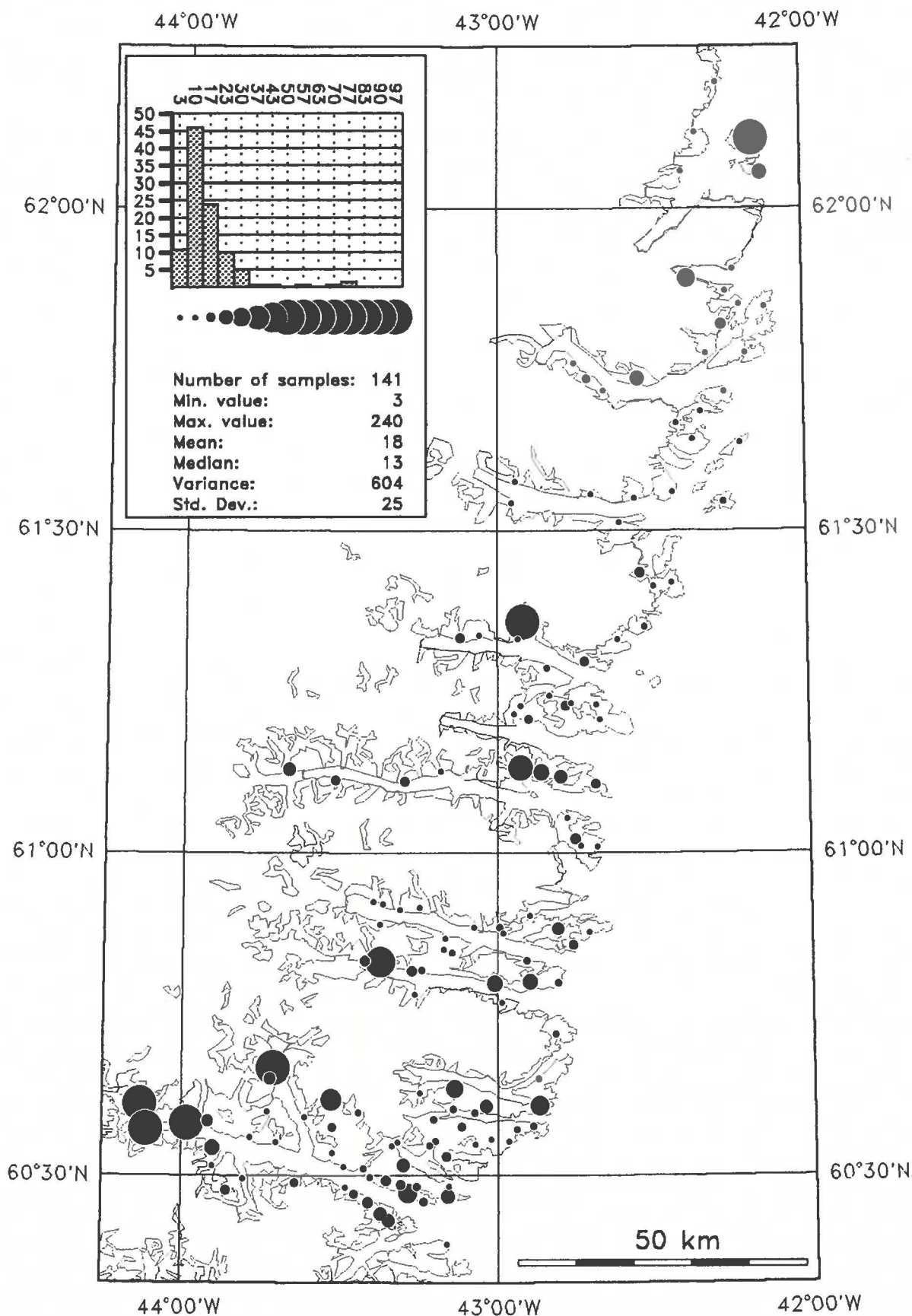


Fig. 24

La (ppm) in stream sediment

Instrumental Neutron Activation

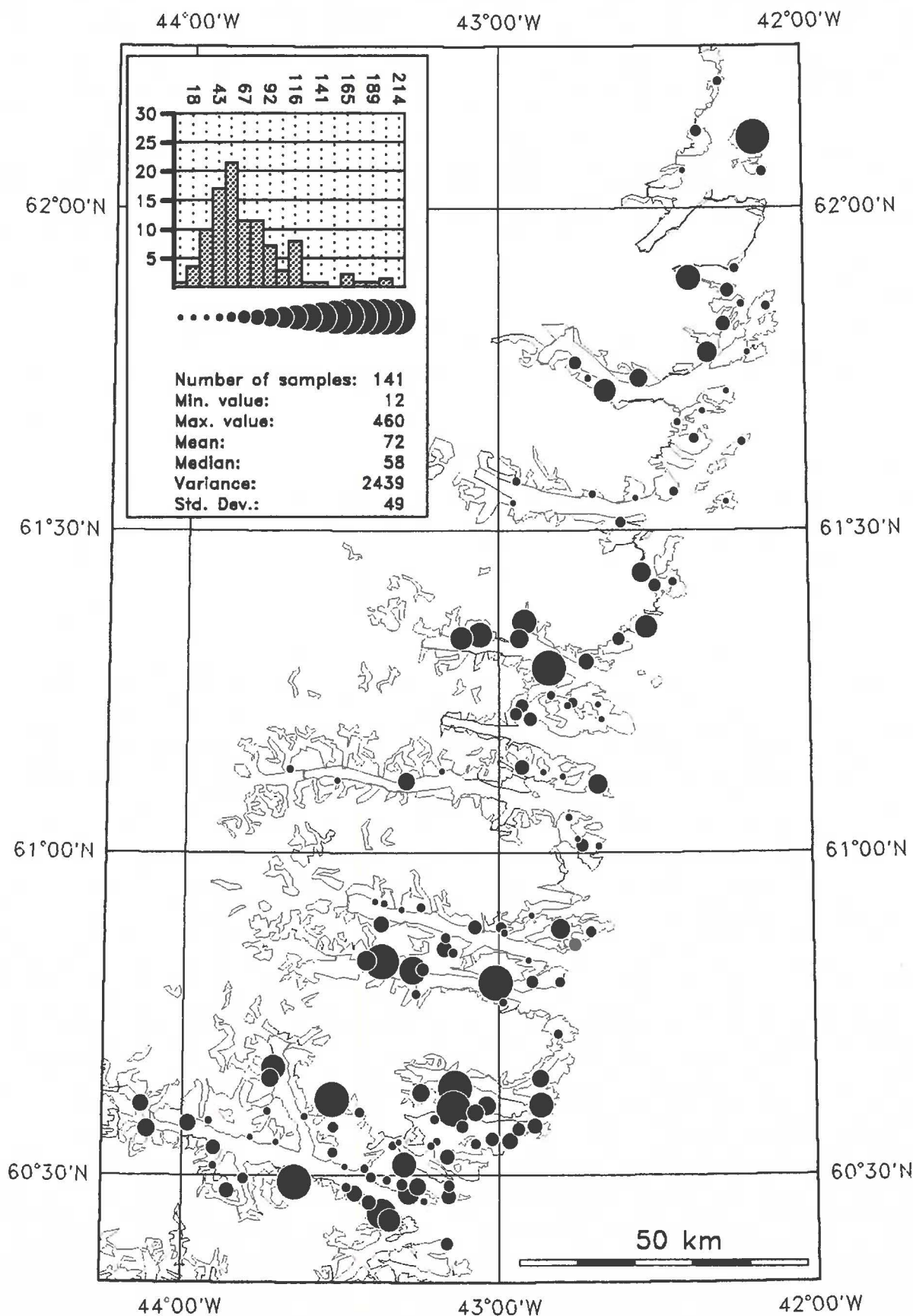


Fig. 25

Lu (ppm) in stream sediment



Instrumental Neutron Activation

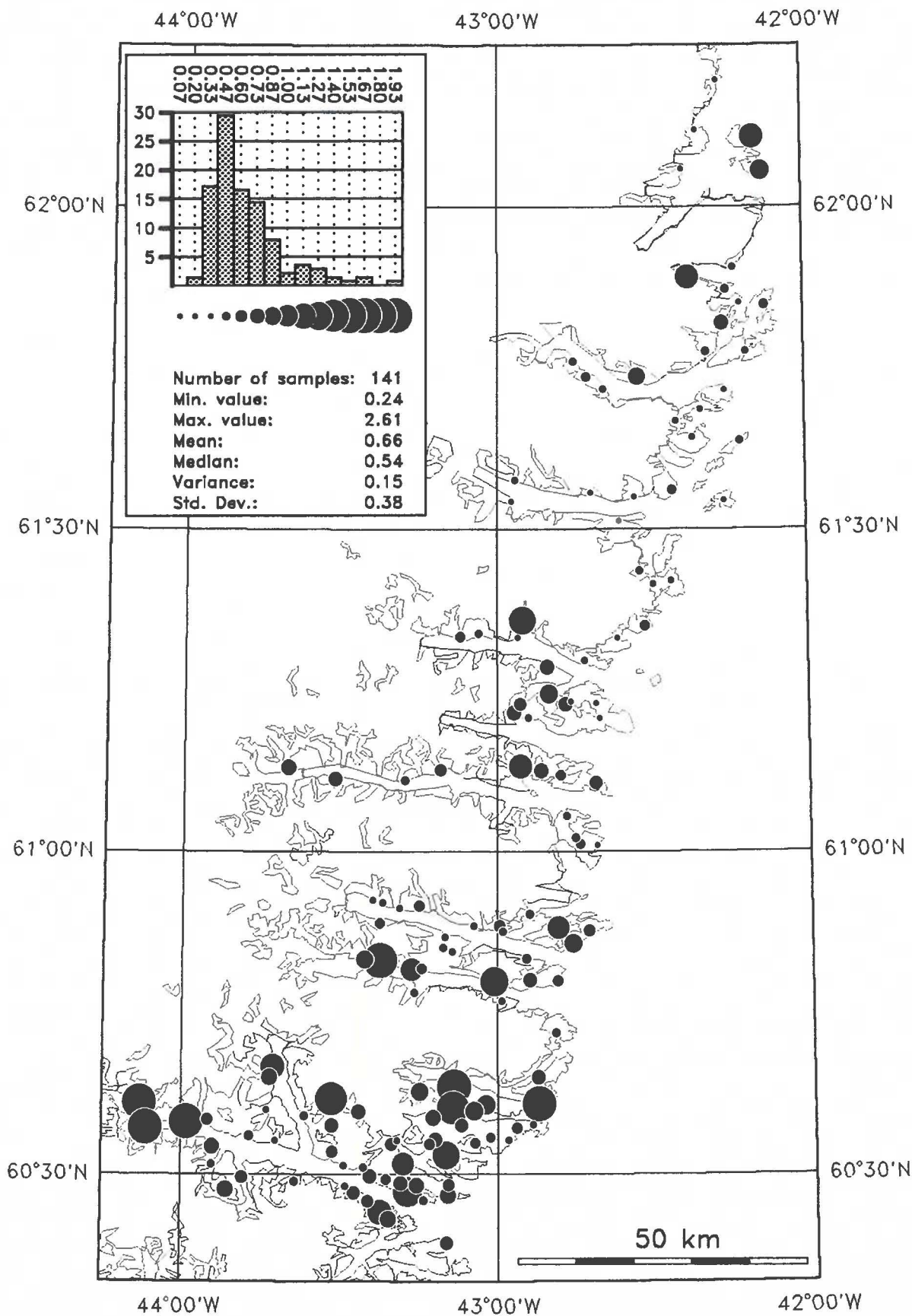


Fig. 26

Mo (ppm) in stream sediment



Instrumental Neutron Activation

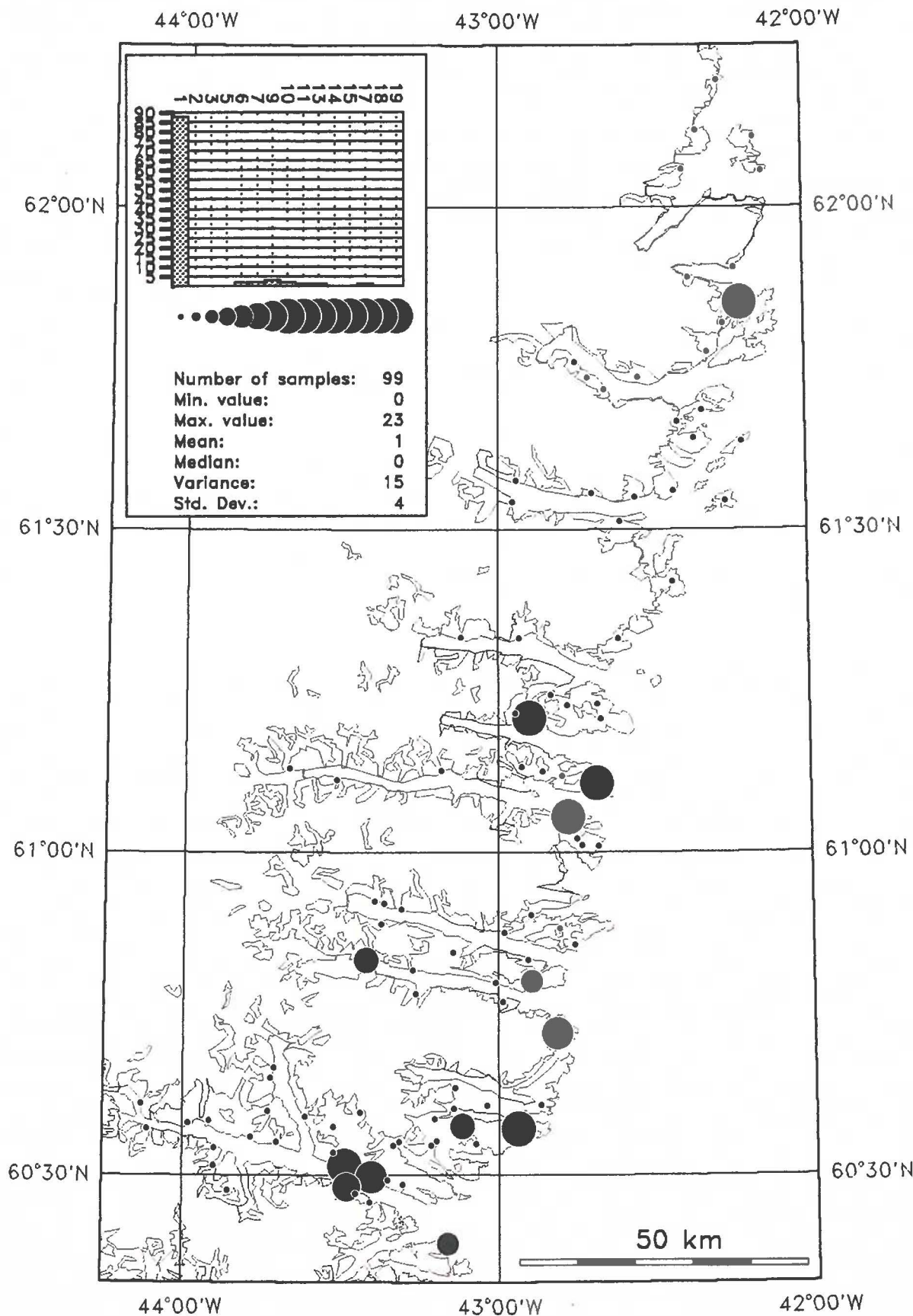


Fig. 27

Nb (ppm) in stream sediment



X-ray Fluorescence

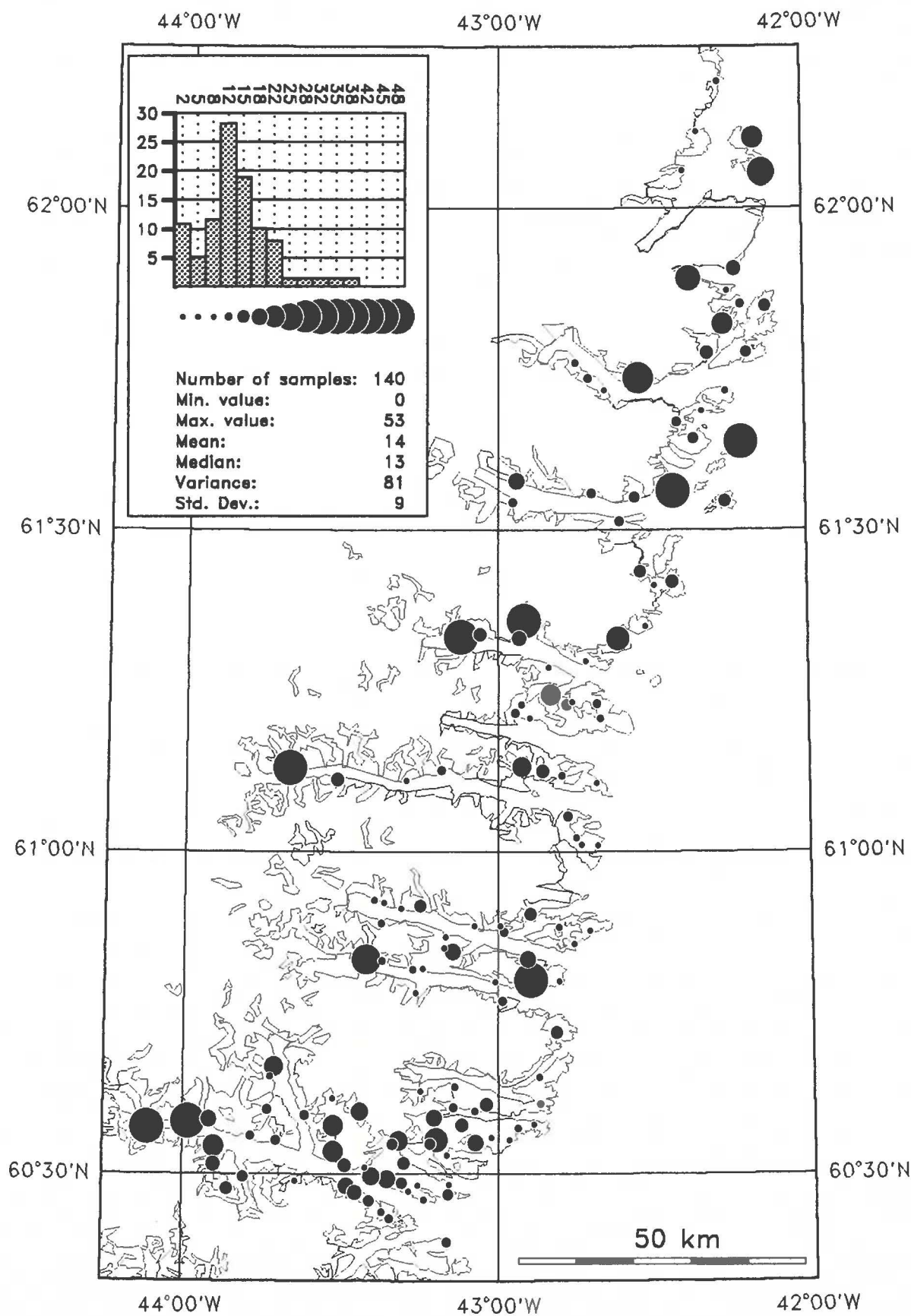


Fig. 28

Nd (ppm) in stream sediment

Instrumental Neutron Activation

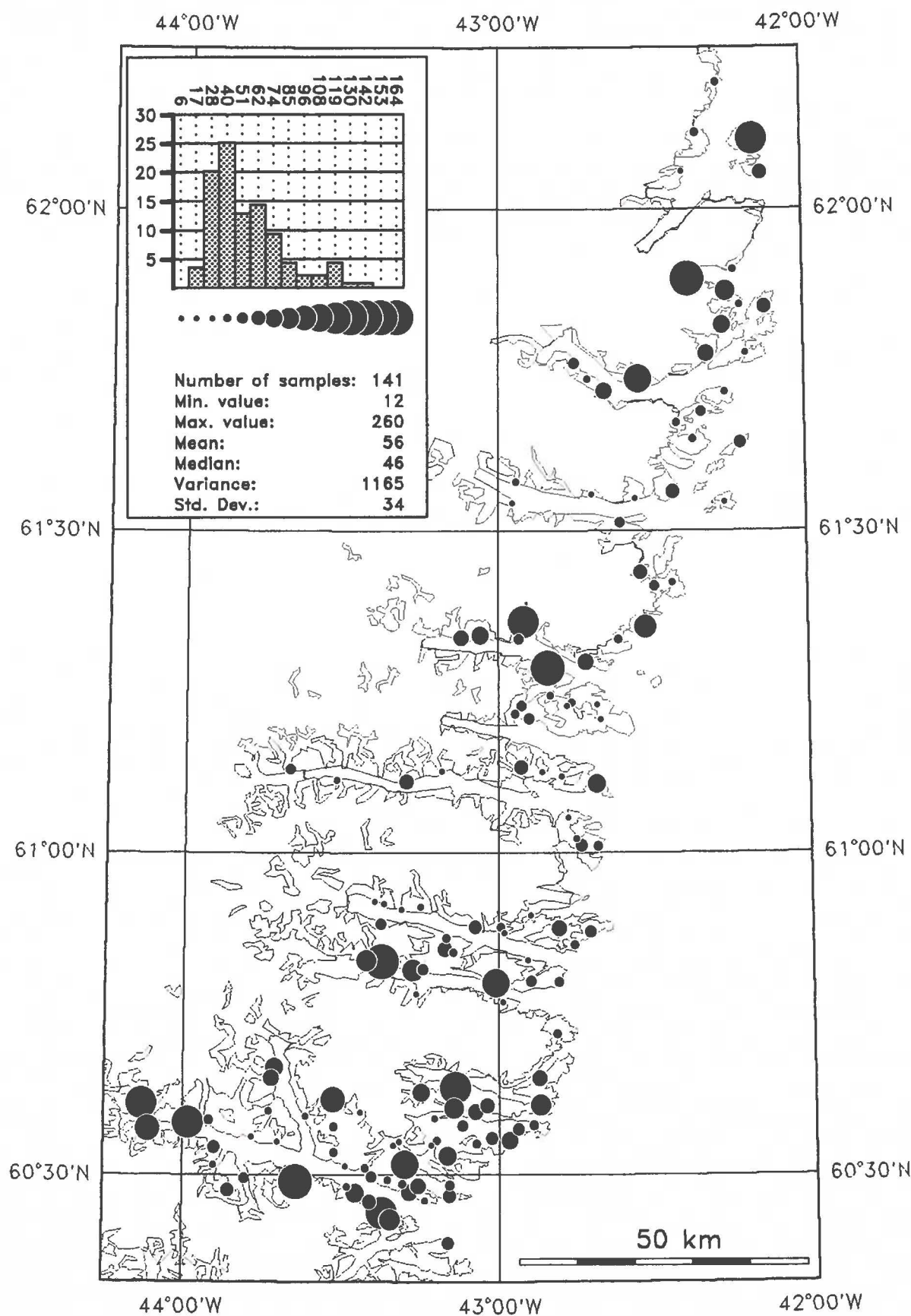


Fig. 29

Ni (ppm) in stream sediment



X-ray Fluorescence

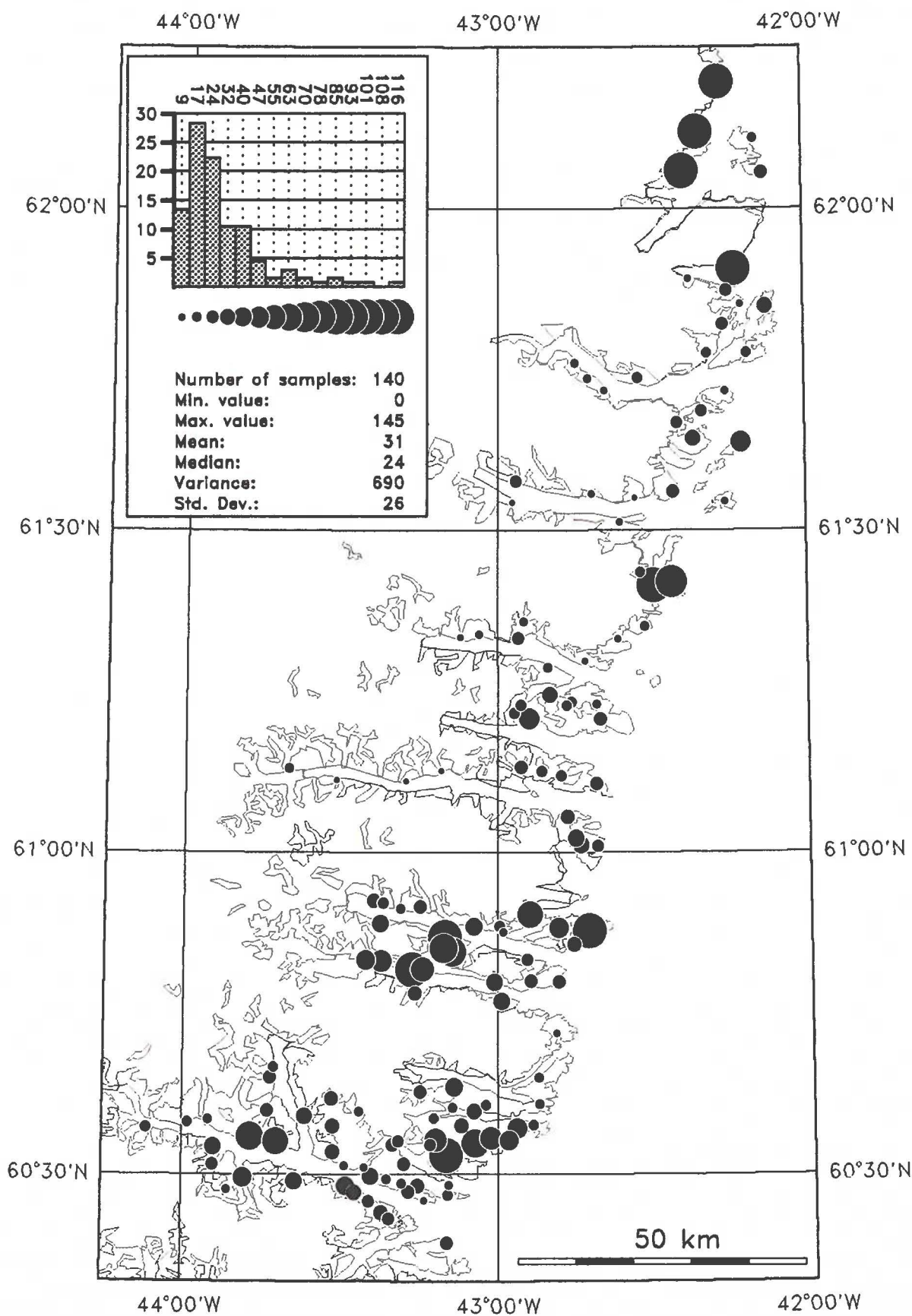


Fig. 30

Pb (ppm) in stream sediment



X-ray Fluorescence

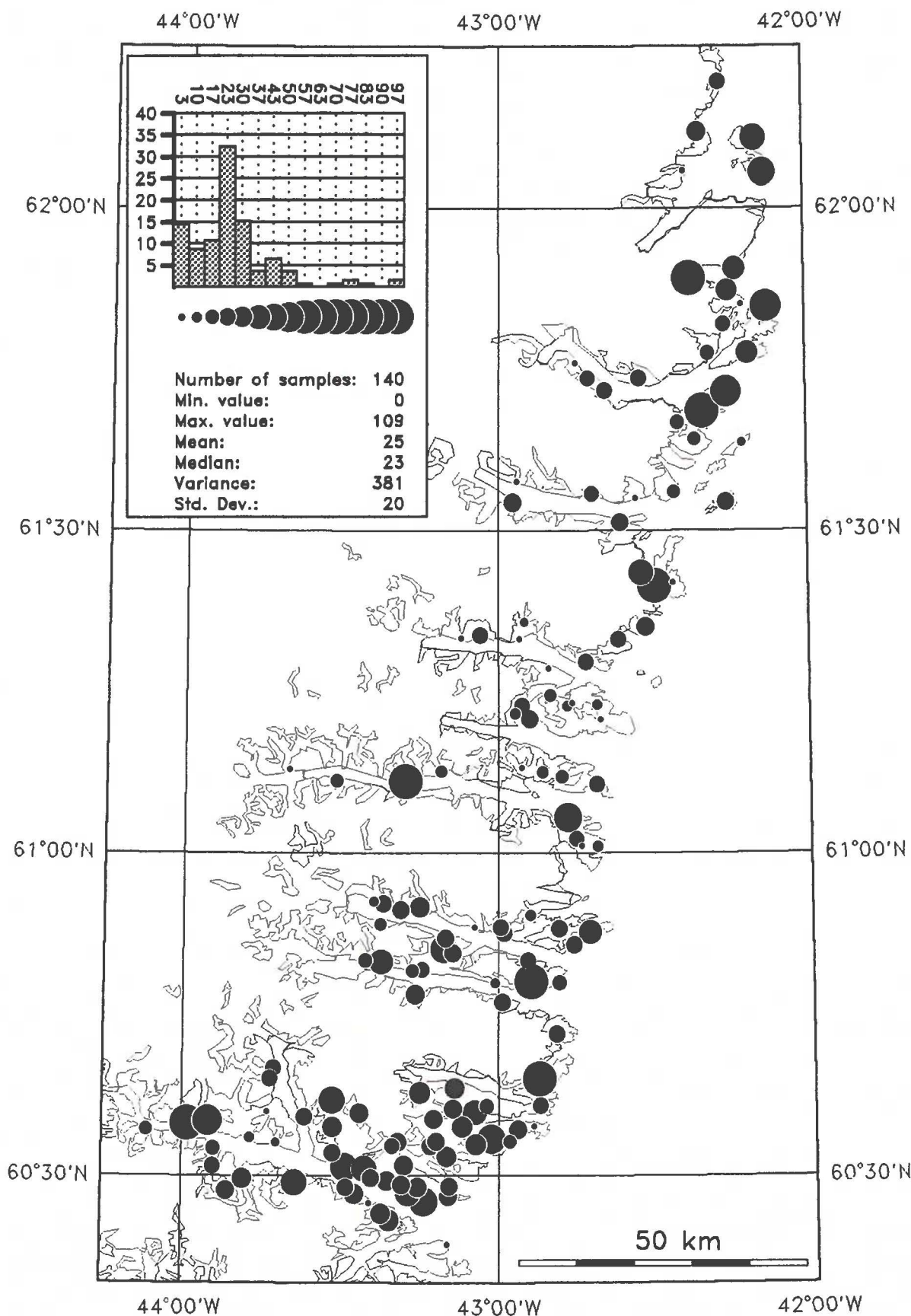


Fig. 31

Rb (ppm) in stream sediment



X-ray Fluorescence

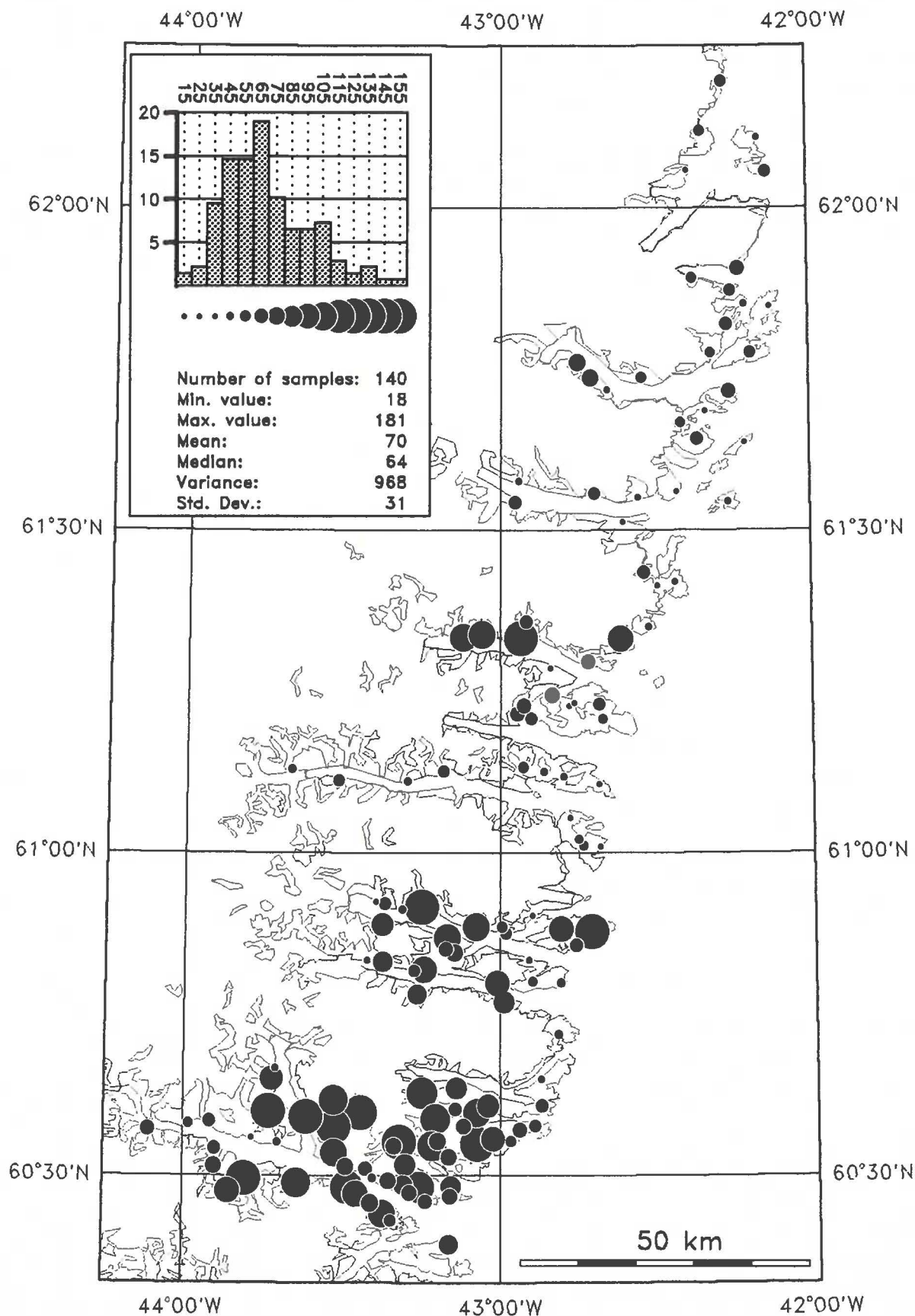


Fig. 32

Sb (ppm) in stream sediment



Instrumental Neutron Activation

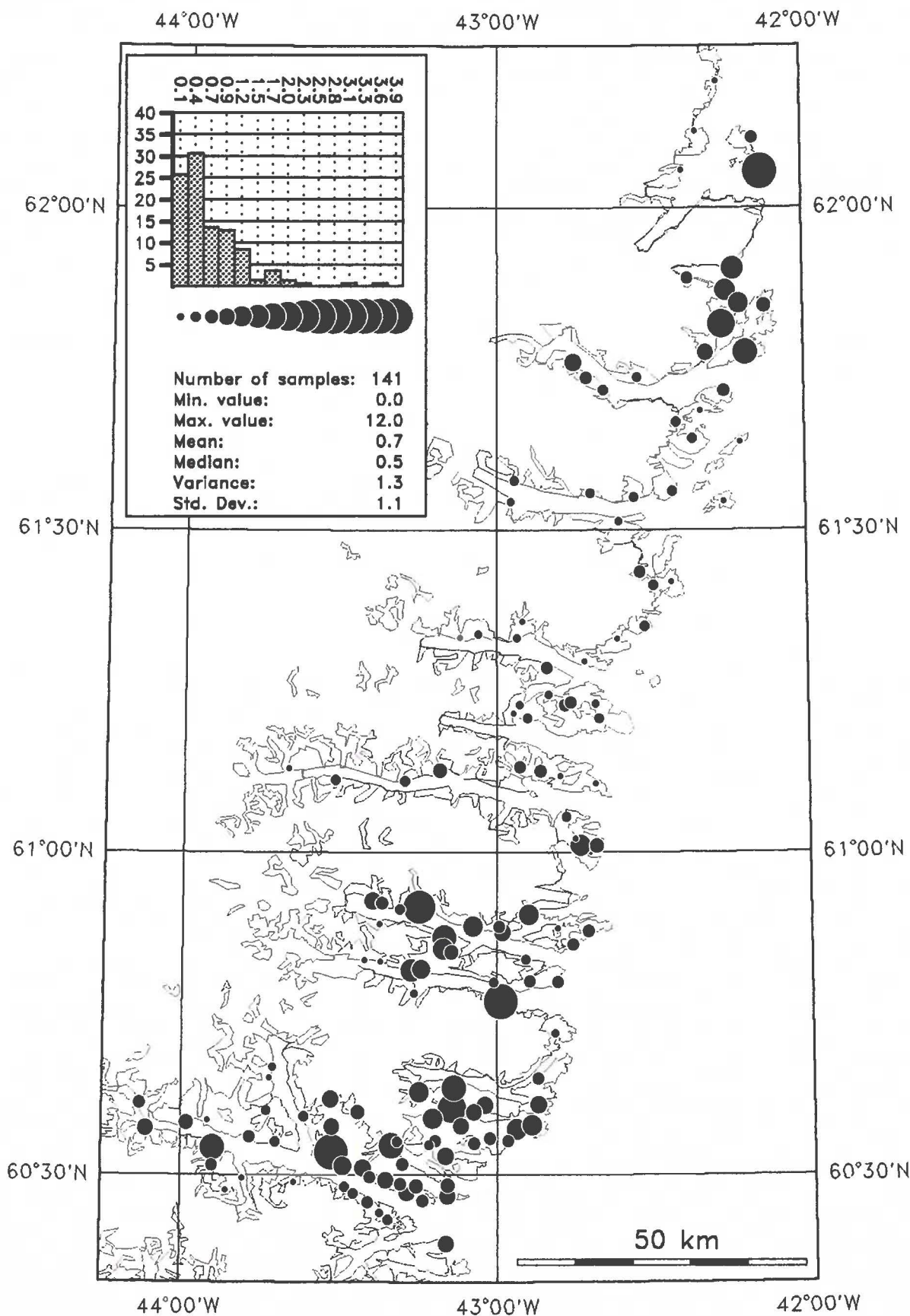


Fig. 33

Sc (ppm) in stream sediment



Instrumental Neutron Activation

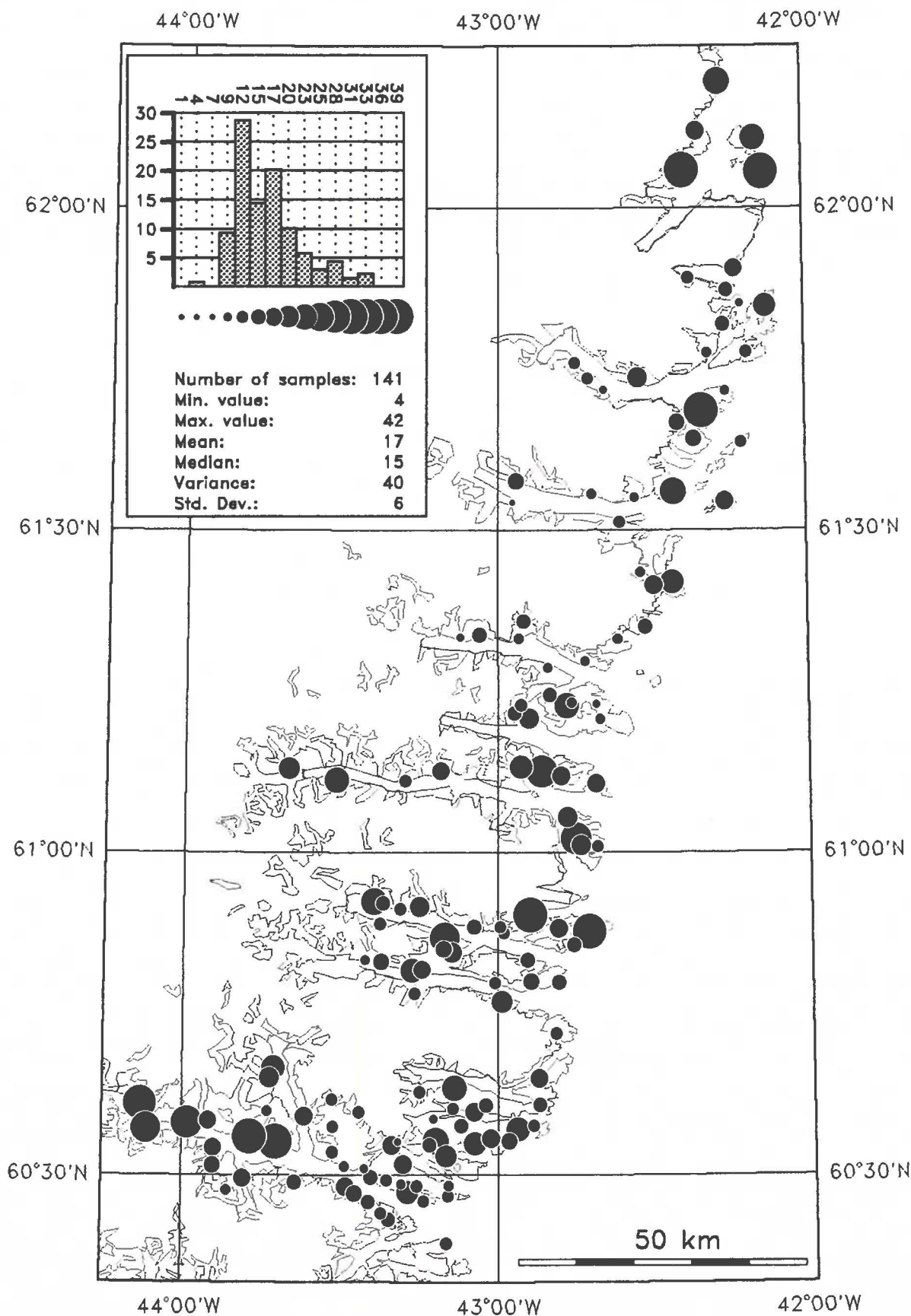


Fig. 34

Sm (ppm) in stream sediment



Instrumental Neutron Activation

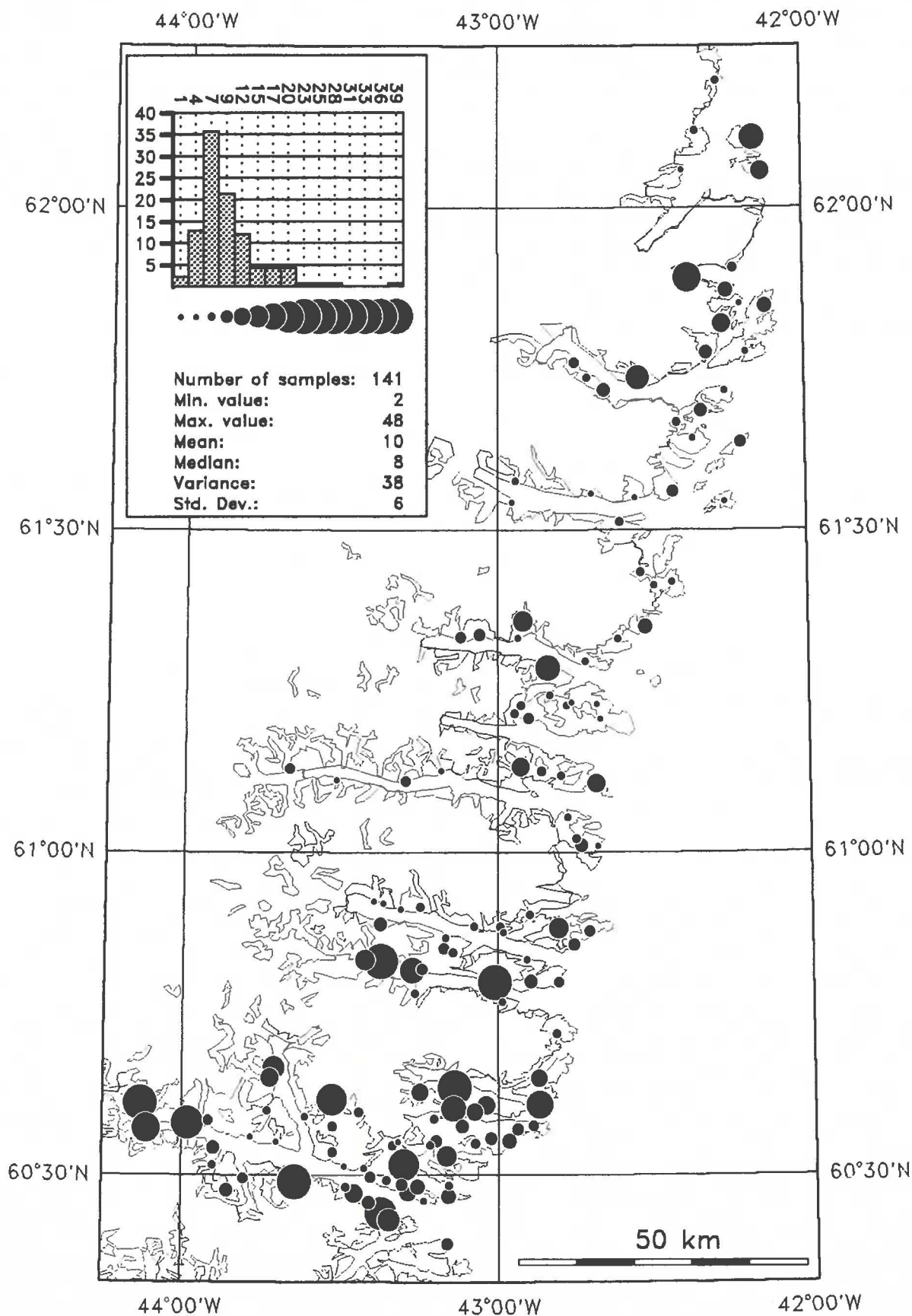


Fig. 35

Sr (ppm) in stream sediment

X-ray Fluorescence

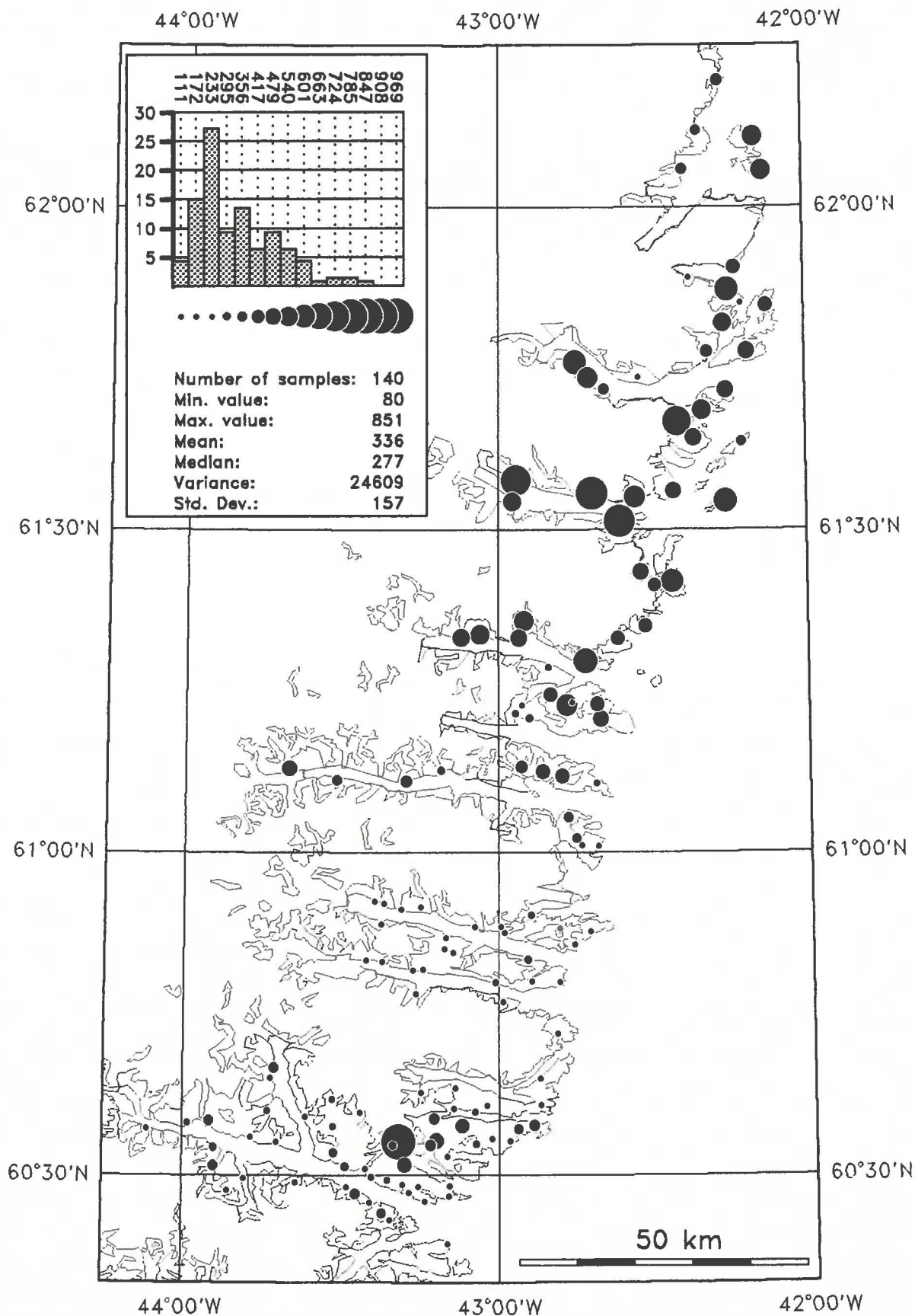


Fig. 36

Th (ppm) in stream sediment

Instrumental Neutron Activation

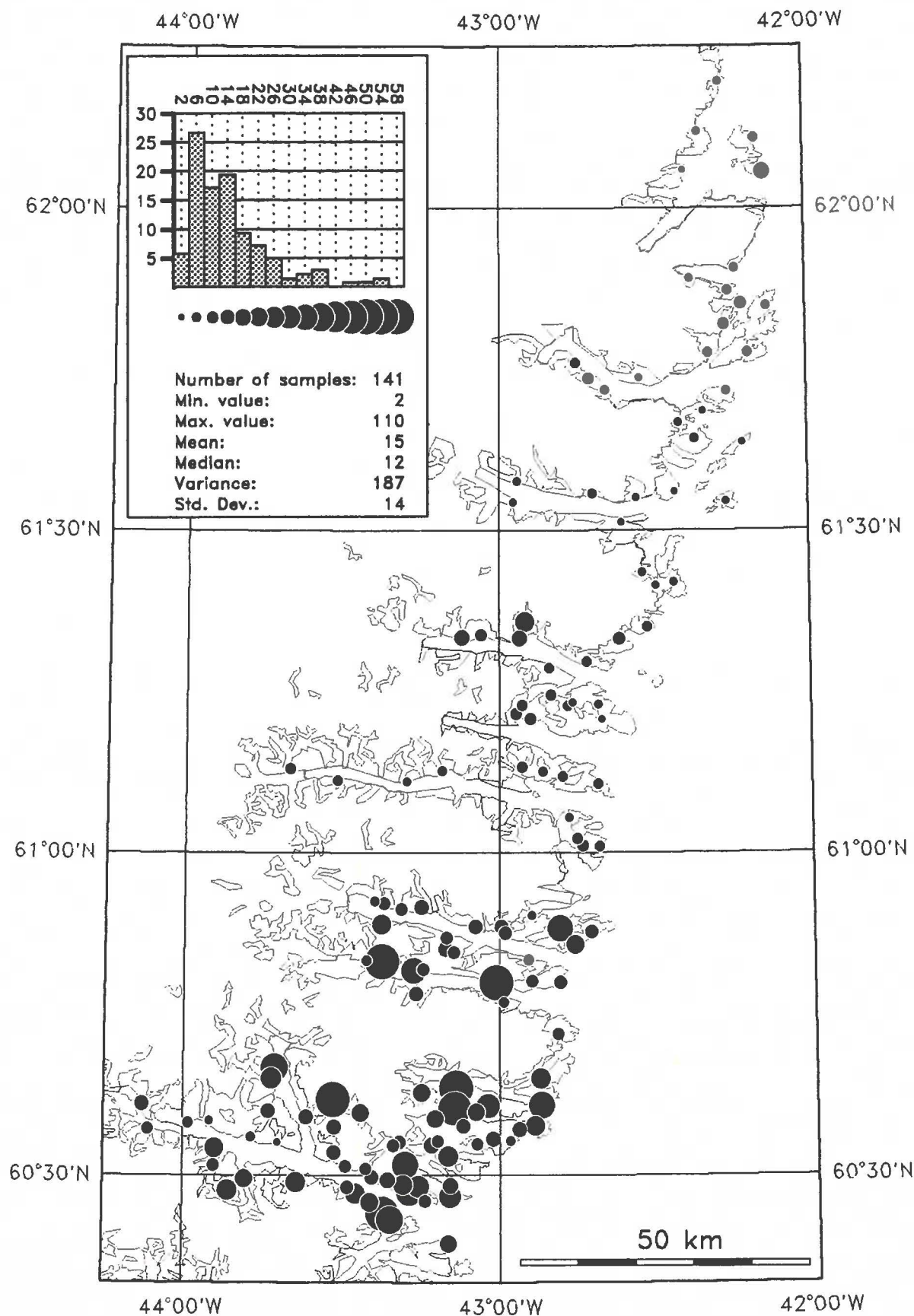


Fig. 37

U (ppm) in stream sediment



Instrumental Neutron Activation

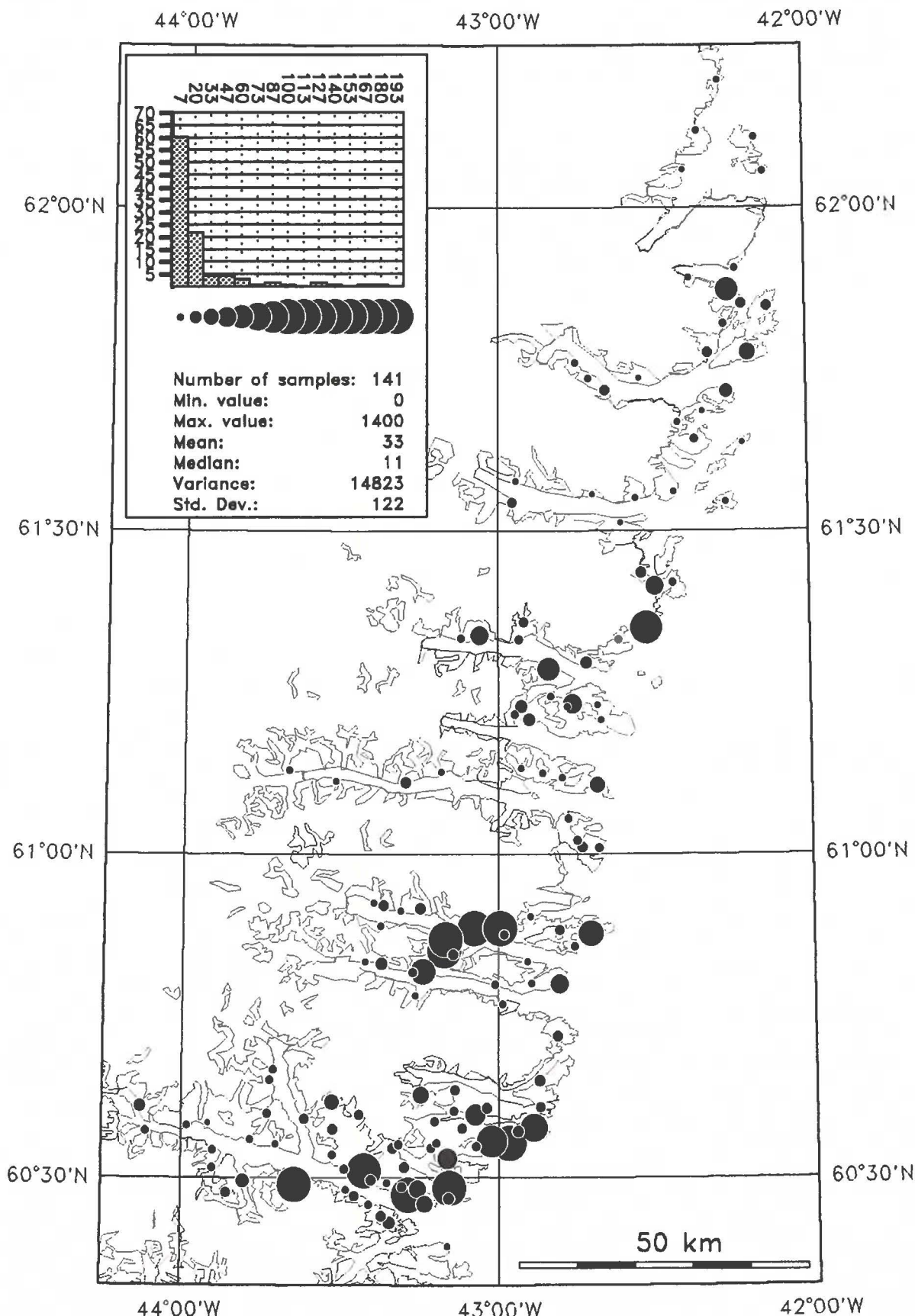
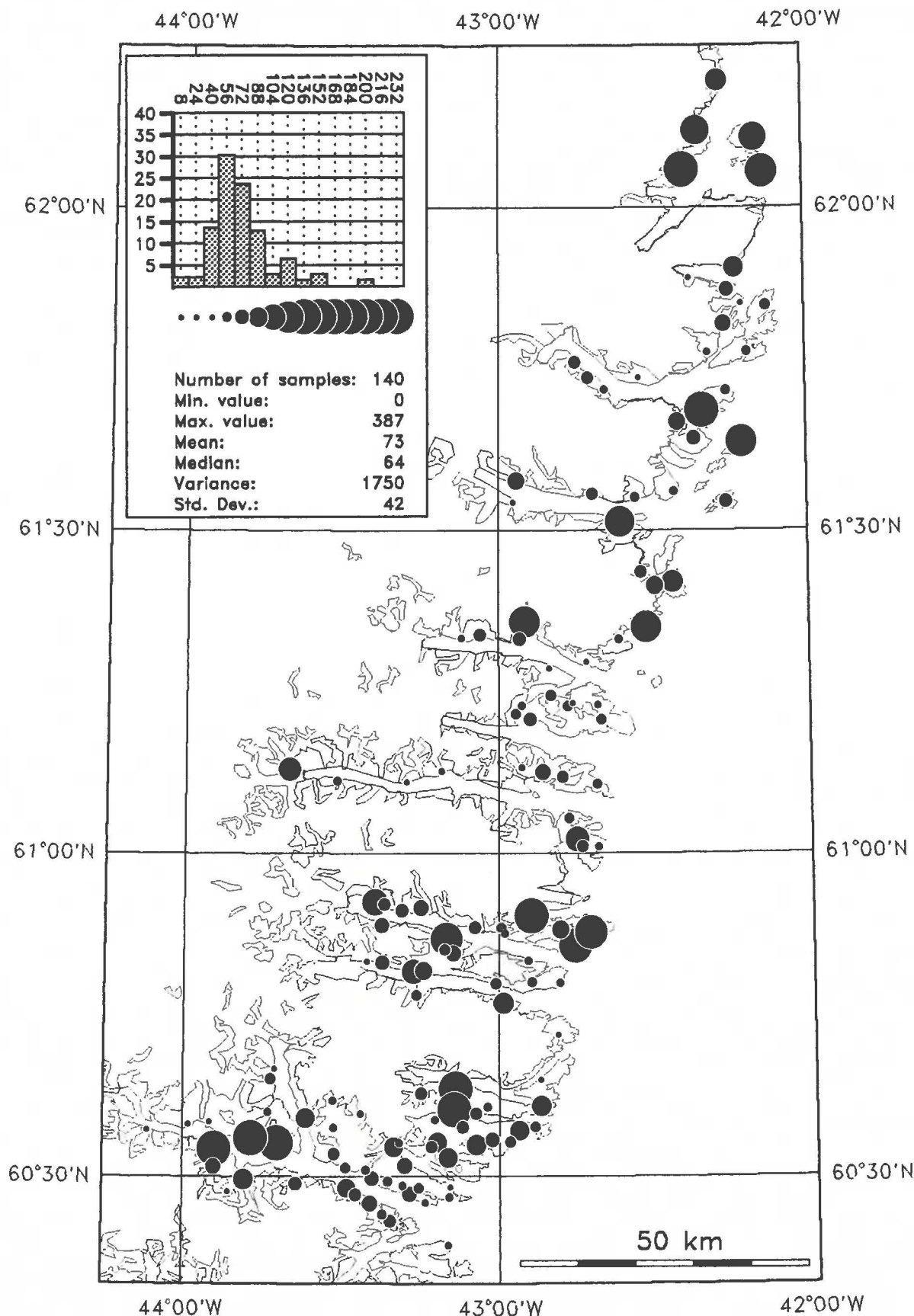


Fig. 38

V (ppm) in stream sediment



X-ray Fluorescence



W (ppm) in stream sediment



Instrumental Neutron Activation

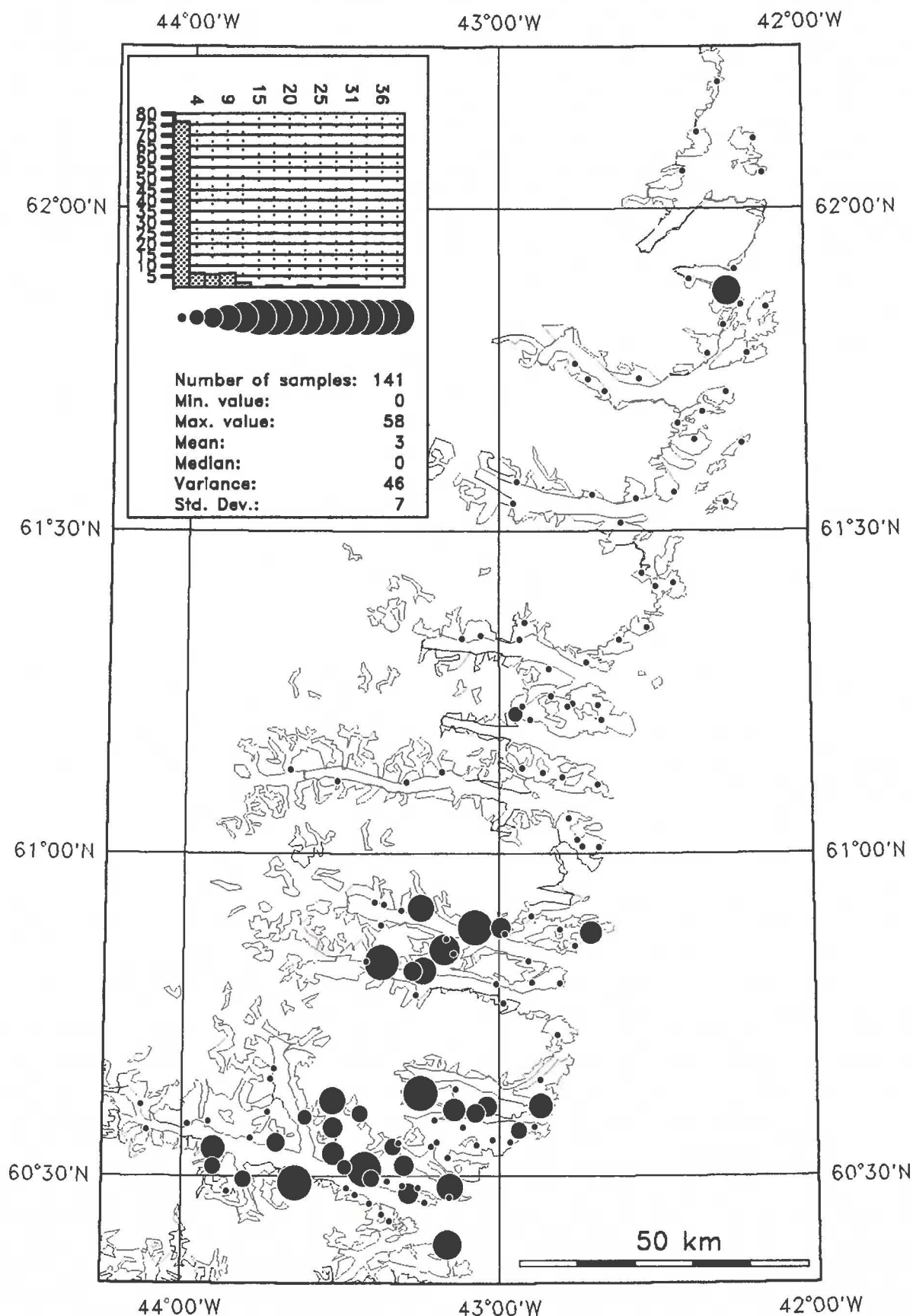


Fig. 40

Y (ppm) in stream sediment

X-ray Fluorescence

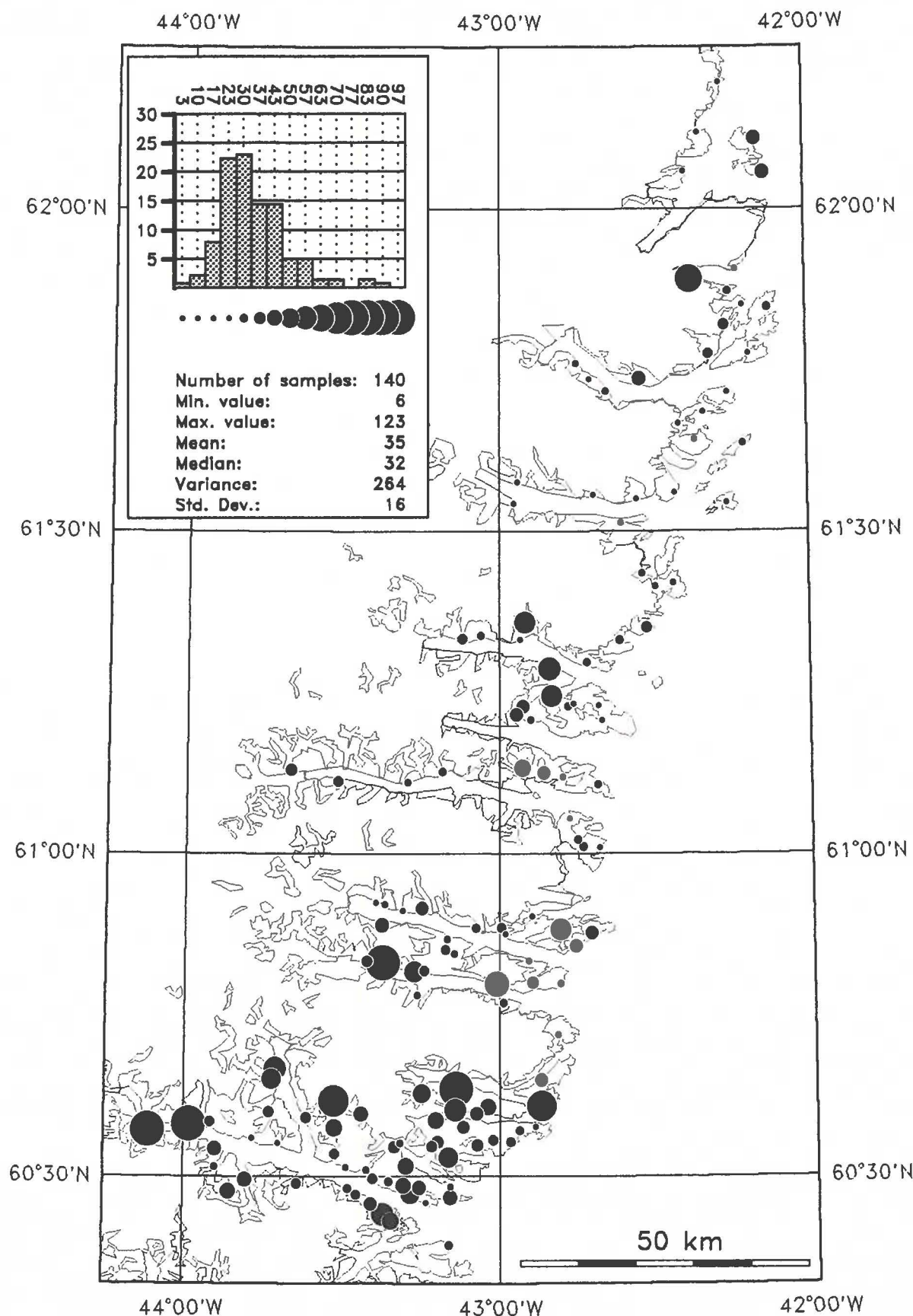


Fig. 41

Yb (ppm) in stream sediment



Instrumental Neutron Activation

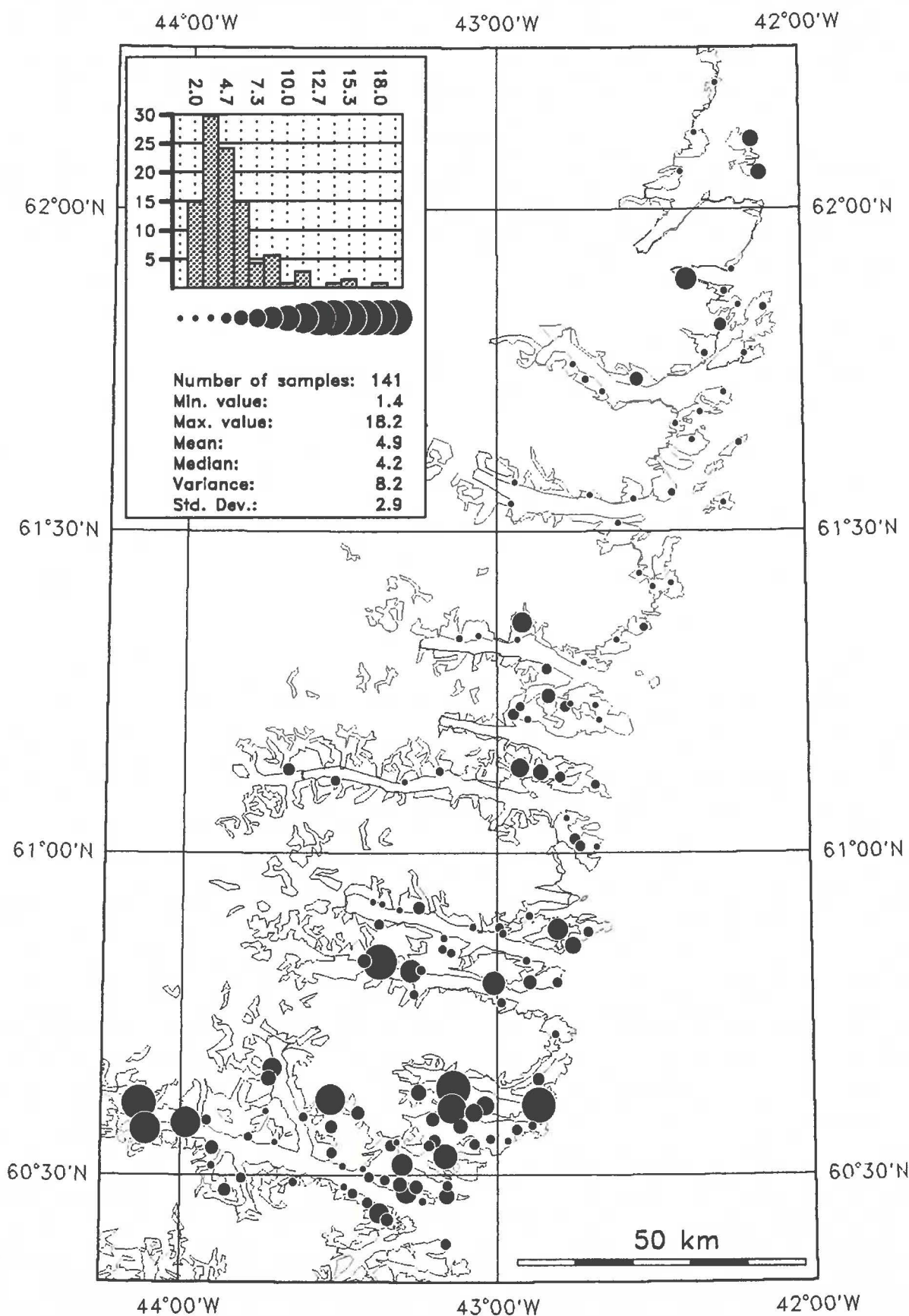


Fig. 42

Zn (ppm) in stream sediment



X-ray Fluorescence

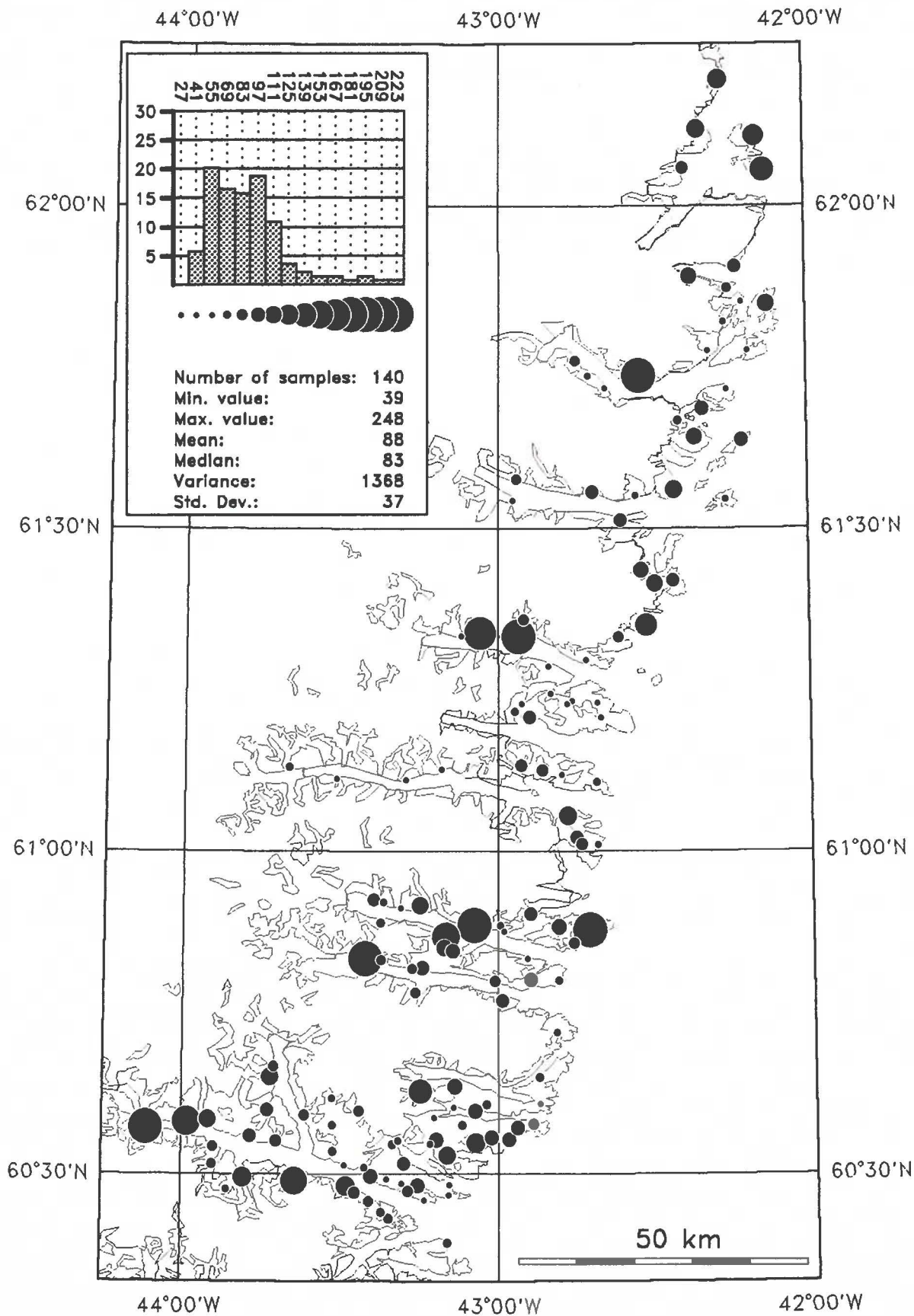


Fig. 43

Zr (ppm) in stream sediment



X-ray Fluorescence

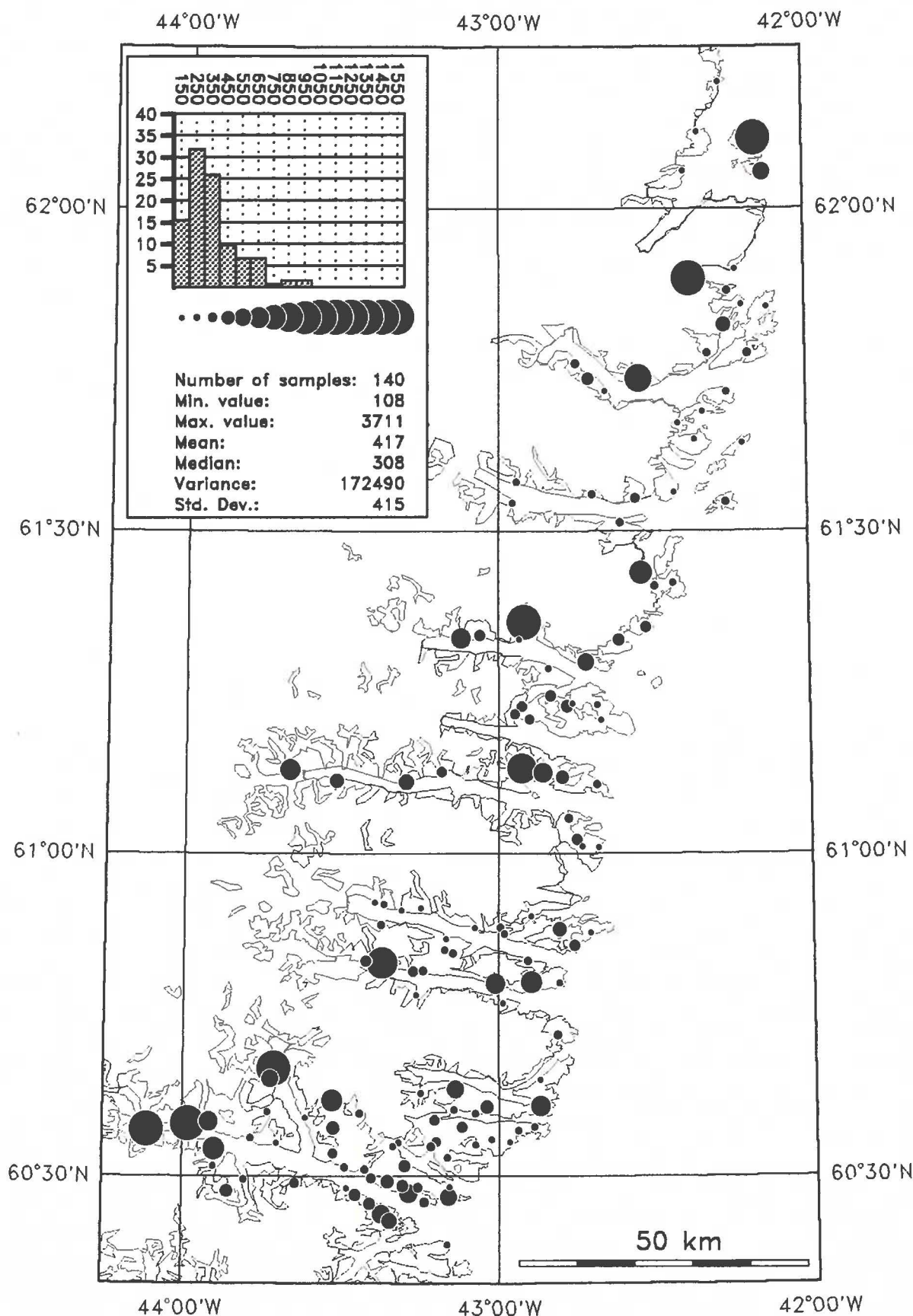


Fig. 44

Total radiation (counts per sec.)



Scintillometry

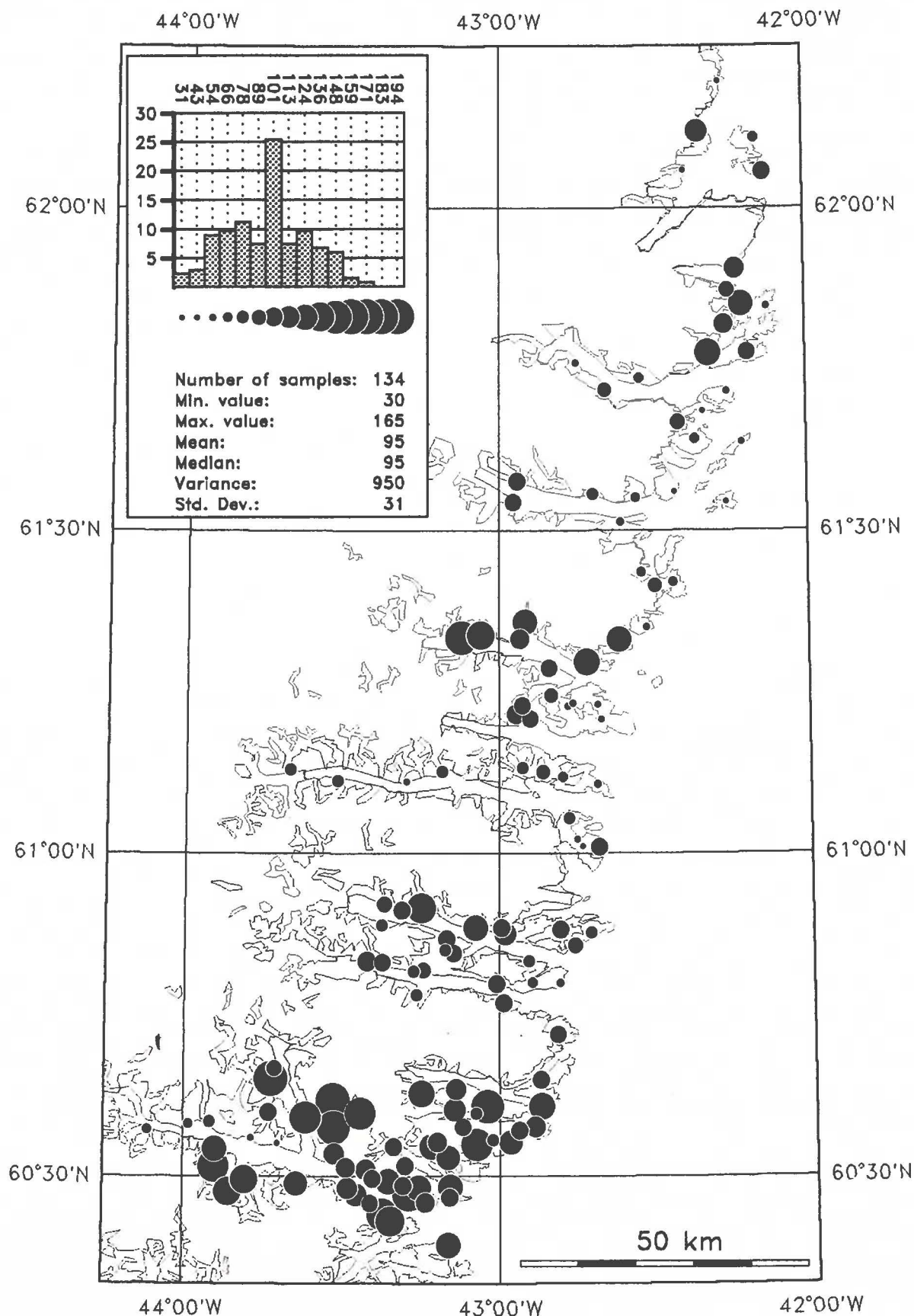


Fig. 45

Conductivity of stream water

(micro sievert)

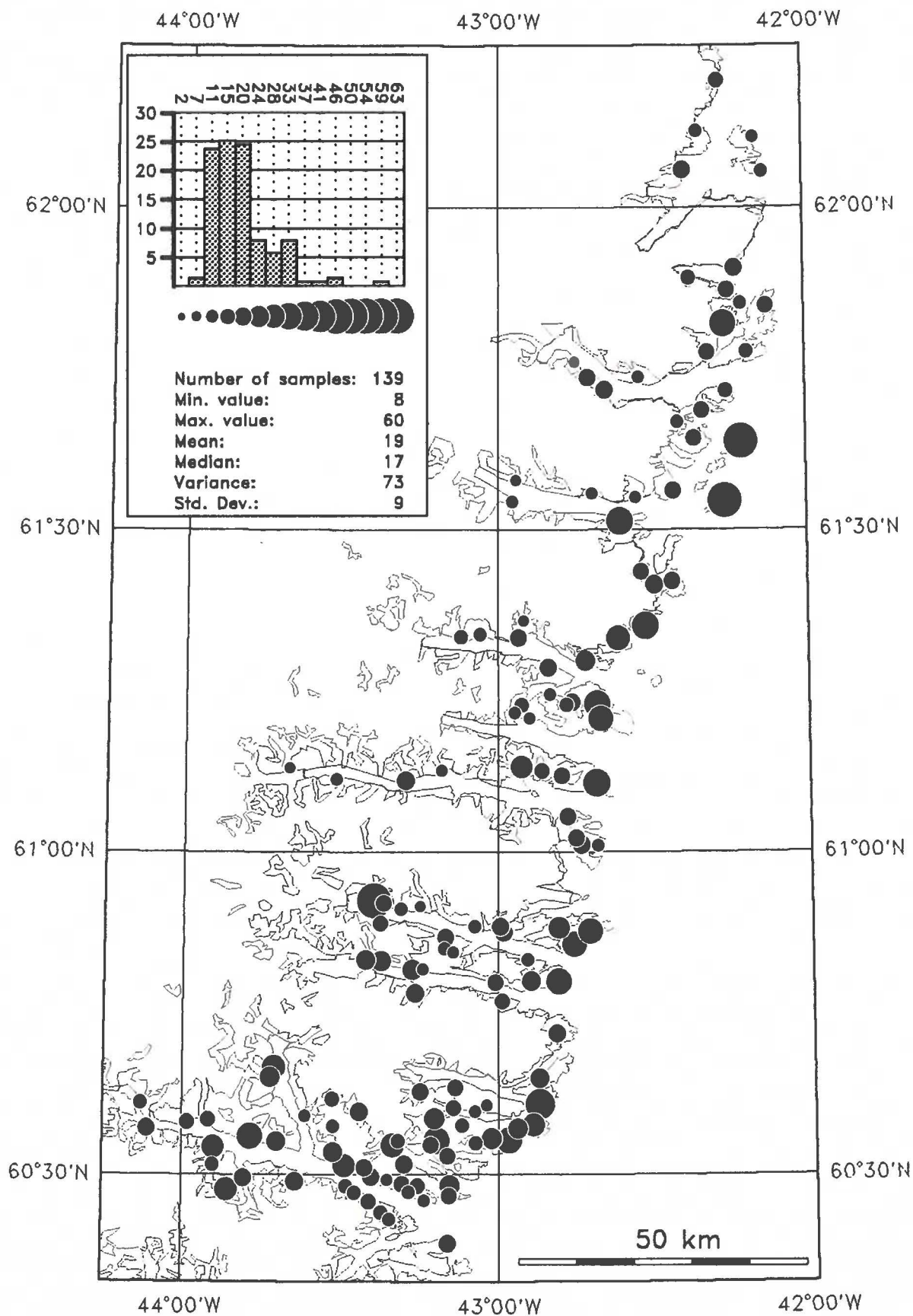


Fig. 46

F (ppb) in stream water



Ion sensitive electrode

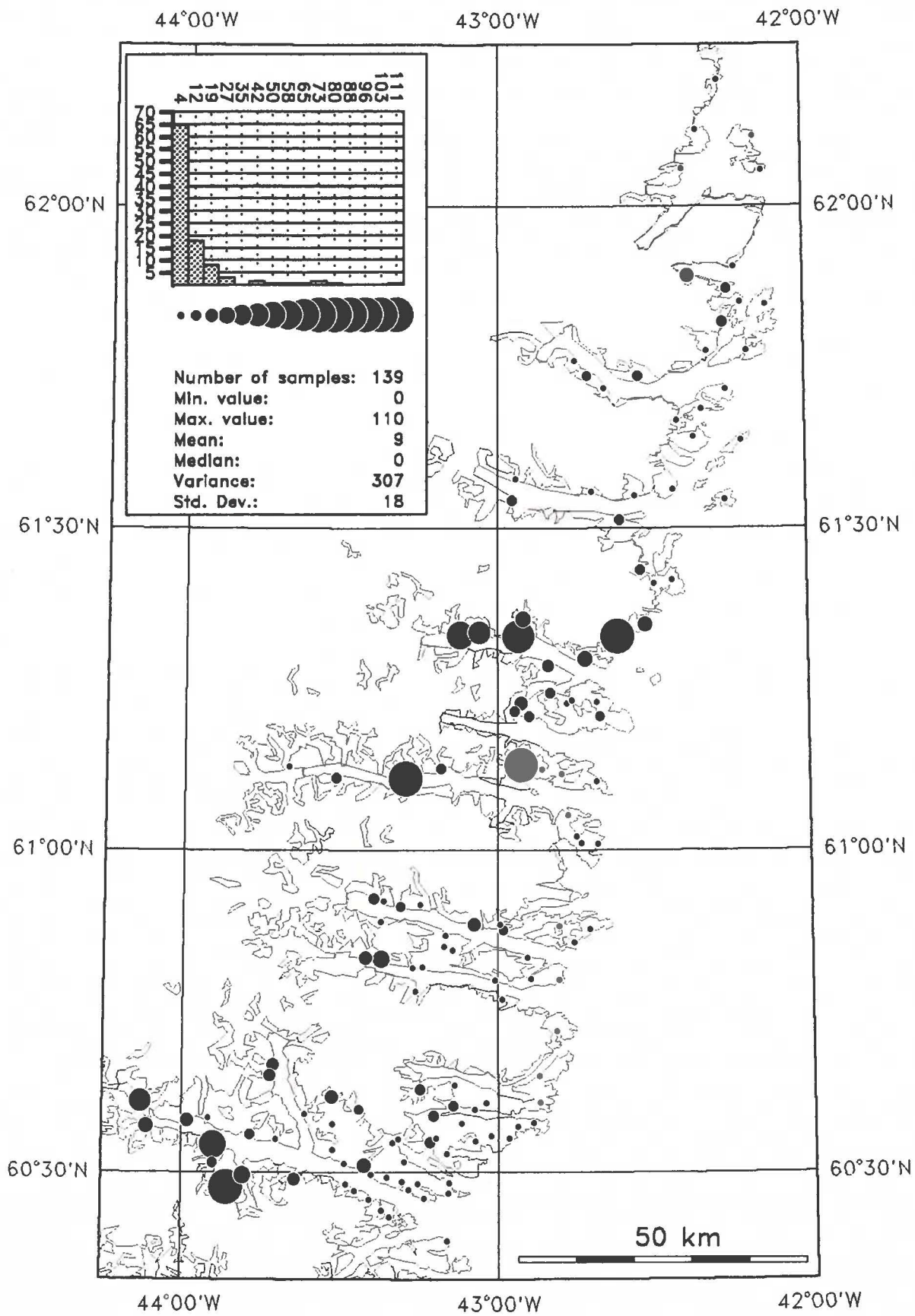


Fig. 47

Stream sediment anomalies

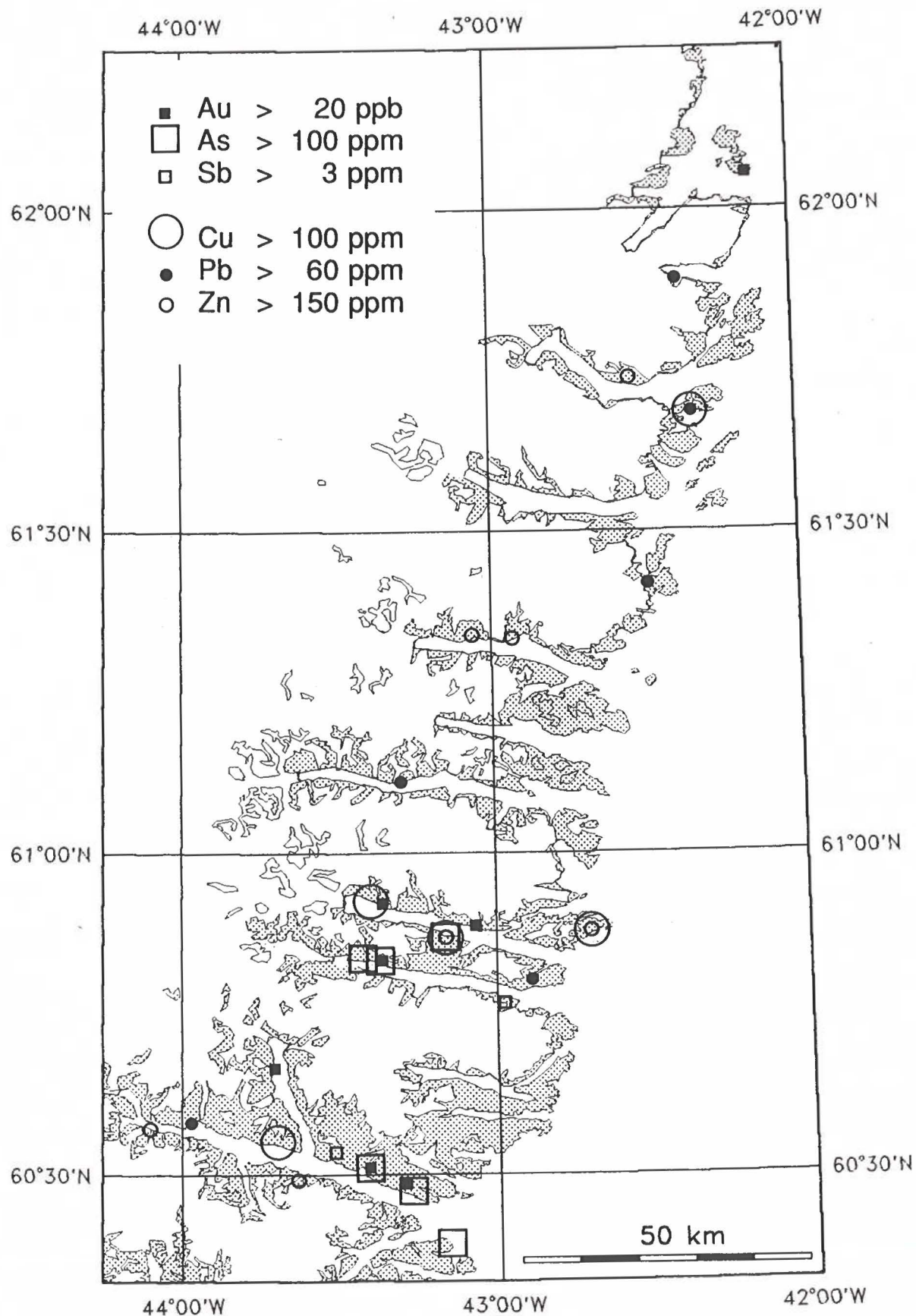


Fig. 48

Stream sediment anomalies

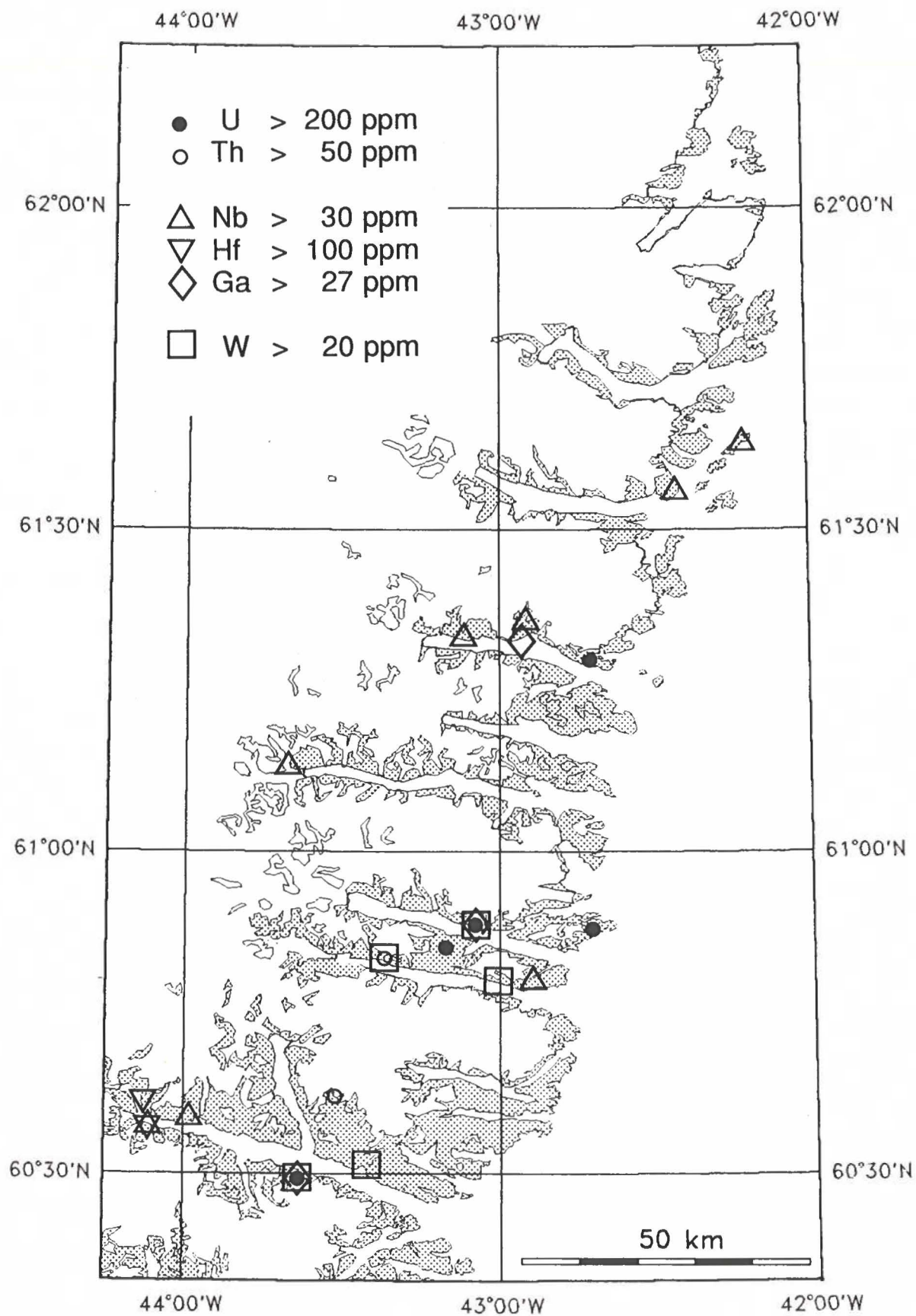


Fig. 49

